medRxiv preprint doi: https://doi.org/10.1101/2020.06.08.20125757; this version posted June 9, 2020. The copyright holder for this preprint (which was not certified by peer review) is the author/funder, who has granted medRxiv a license to display the preprint in perpetuity. It is made available under a CC-BY 4.0 International license .

The role of socioeconomic status, environment, and temperature in the spatio-temporal distribution of the first Chikungunya epidemic in the city of Rio de Janeiro, Brazil

Laís Picinini Freitas[1]*, Alexandra M. Schmidt[2], William Cossich[3], Oswaldo Gonçalves Cruz[4], Marilia Sá Carvalho[4]

[1] Programa de Pós-Graduação em Epidemiologia em Saúde Pública, Escola Nacional de Saúde Pública Sergio Arouca (ENSP), Oswaldo Cruz Foundation, Rio de Janeiro, Brazil

[2] Department of Epidemiology, Biostatistics and Occupational Health, McGill University, Montreal, Canada

[3] Department of Physics and Astronomy, University of Bologna, Bologna, Italy

[4] Programa de Computação Científica (PROCC), Oswaldo Cruz Foundation, Rio de Janeiro, Brazil

* Corresponding author

E-mail: lais.picinini.freitas@gmail.com (LPF)

NOTE: This preprint reports new research that has not been certified by peer review and should not be used to guide clinical practice.

medRxiv preprint doi: https://doi.org/10.1101/2020.06.08.20125757; this version posted June 9, 2020. The copyright holder for this preprint (which was not certified by peer review) is the author/funder, who has granted medRxiv a license to display the preprint in perpetuity. It is made available under a CC-BY 4.0 International license .

Abstract

Chikungunya is an *Aedes*-borne disease therefore its dynamics are impacted by the vector's ecology. We analysed the spatio-temporal distribution of the first chikungunya epidemic in Rio de Janeiro, estimating the effect of the socioeconomic and environmental factors as proxies of mosquitoes abundance. We fitted spatial models using notified cases counts by neighbourhood and week. To estimate the instantaneous and the memory effect of the temperature we used a transfer function. There were 13627 chikungunya cases in the study period. The sociodevelopment index, especially in the beginning of the epidemic, was inversely associated with the risk of cases, whereas the green area proportion effect was null for most weeks. The temperature increased the risk of chikungunya in most areas and this effect propagated for longer where the epidemic was concentrated. Factors related to the *Aedes* mosquitoes contribute to understanding the spatio-temporal dynamics of urban arboviral diseases.

Key-words: chikungunya, spatial model, epidemiology

medRxiv preprint doi: https://doi.org/10.1101/2020.06.08.20125757; this version posted June 9, 2020. The copyright holder for this preprint (which was not certified by peer review) is the author/funder, who has granted medRxiv a license to display the preprint in perpetuity. It is made available under a CC-BY 4.0 International license .

Introduction

The first chikungunya virus (CHIKV) epidemic in Rio de Janeiro city, the second most populated city in Brazil and its main tourist destination, occurred in 2016 (de Souza et al., 2018). CHIKV is transmitted to humans by the same vectors as dengue viruses (DENV), the *Aedes* mosquitoes (WHO, 2017). Vector-control activities have not prevented Rio de Janeiro from being endemic for dengue for years, nor from having experienced large dengue epidemics, in general, every three to four years (Honório et al., 2009c; Nogueira et al., 1999; Santos et al., 2019).

For an arbovirus epidemic to occur three main elements are necessary, represented by the blue circle in Figure 1: mosquito population, susceptible human population, and the virus circulating (Kuno, 1995; Randolph and Rogers, 2010; Teixeira et al., 2009). The *Ae. aegypti* mosquito is present all over the city of Rio de Janeiro, facilitating a new arbovirus is established and spread quickly. Despite sharing the same vector, CHIKV and DENV belong to different families, which means that previous immunity to DENV does not cross-react with CHIKV and the population of Rio de Janeiro could be considered equally naïve to CHIKV before 2016. Therefore, the occurrence of local transmission was conditioned by the entry of the virus.

Figure 1. A theoretical model for a chikungunya epidemic in a given region. Direct associations are represented by black arrows and indirect associations by red arrows. The blue area includes the necessary elements for the epidemic to occur.

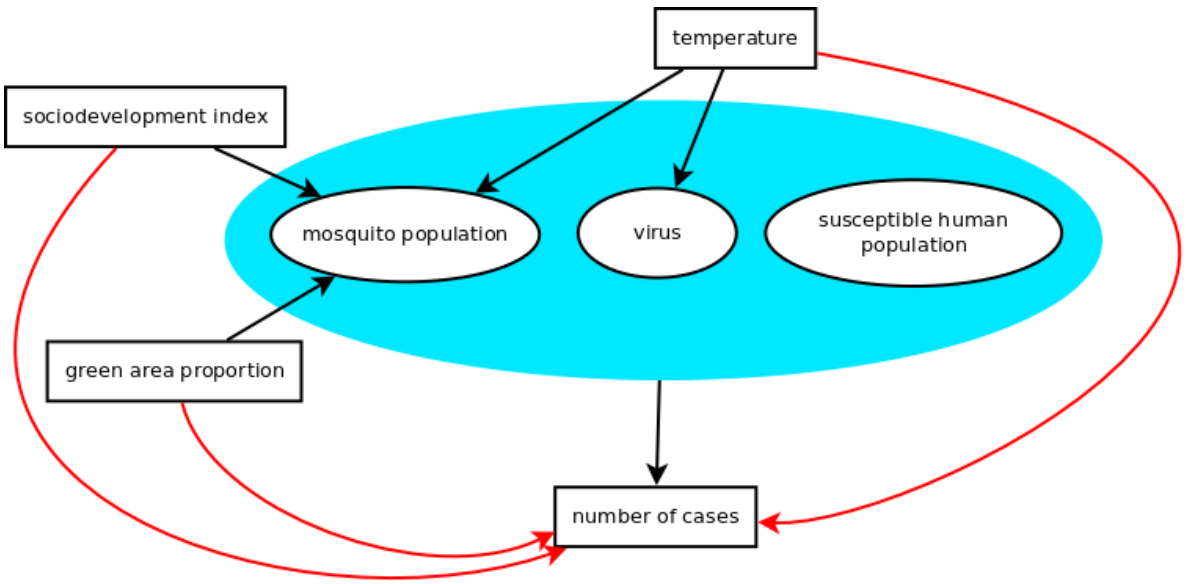

medRxiv preprint doi: https://doi.org/10.1101/2020.06.08.20125757; this version posted June 9, 2020. The copyright holder for this preprint (which was not certified by peer review) is the author/funder, who has granted medRxiv a license to display the preprint in perpetuity. It is made available under a CC-BY 4.0 International license .

Reliable data on vector population, susceptible human population, and time of the entry of the virus, are not available at the intra-urban level in Rio de Janeiro city. Therefore, socioeconomic and environmental factors that have a direct effect (represented by black arrows in Figure 1) on the unmeasured elements can be considered to understand the spatio-temporal dynamics of the chikungunya epidemic by estimating their indirect association (represented by red arrows in Figure 1) with the number of cases. The mosquito population varies within the city and with time, as the mosquito ecology is affected by environmental factors such as the level of urbanization and temperature. *Ae. aegypti* mosquitoes are highly adapted to urban settings, and the proportion of green area is inversely correlated with the level of urbanization (Rosa-Freitas et al., 2010). The socioeconomic status impacts the mosquito population as disorderly urbanization and inadequate sanitary conditions favour the presence of the mosquito most common reproduction site: containers filled with water found inside or in the surroundings of domiciles (Carvalho et al., 2017; Honório et al., 2009a). The temperature affects the life cycle and the activity of the mosquito and the incubation period of the virus, with maximal transmission occurring around 26–29°C (Mordecai et al., 2017).

Statistical models are traditional tools to study diseases. In the last decades, models that take into account the spatial dependency structure of the cases have been applied to better understand arboviral diseases epidemics (Carvalho et al., 2020; Lowe et al., 2011, 2018b), and the application of such models for intra-urban settings is growing more recently (Martínez-Bello et al., 2018, 2017; McHale et al., 2019; Teixeira and Cruz, 2011). Adjacent areas supposedly share similar characteristics. The inclusion of a (latent) spatial random effect, after adjusting for available covariates, accounts for both the spatial structure and unmeasurable factors (Morris et al., 2019). We applied spatial models, more specifically, intrinsic conditional autoregressive (ICAR) models (Besag, 1974), in which the the latent spatial effect in a given area depends on the spatial effects of

medRxiv preprint doi: https://doi.org/10.1101/2020.06.08.20125757; this version posted June 9, 2020. The copyright holder for this preprint (which was not certified by peer review) is the author/funder, who has granted medRxiv a license to display the preprint in perpetuity. It is made available under a CC-BY 4.0 International license .

the neighbouring areas. We aimed to study the spatio-temporal dynamics of the first chikungunya epidemic in Rio de Janeiro city, exploring the effects of temperature, green area proportion and sociodevelopment index.

Methods

Study site

Rio de Janeiro is the second-largest city in Brazil with 6,3 million inhabitants (2010) and its primary tourist destination. Rio's area is of 1204 km², with 160 neighbourhoods grouped into four large regions (Downtown, South, North and West). These regions are subdivided in 10 health districts called programmatic areas: area 1.0 (Downtown region); areas 2.1 and 2.2 (South region); areas 3.1, 3.2, 3.3 (North region); and areas 4.0, 5.1, 5.2 and 5.3 (West region) (Figure 2).

Figure 2. Rio de Janeiro city by programmatic areas and neighbourhoods, 2010, Brazil.

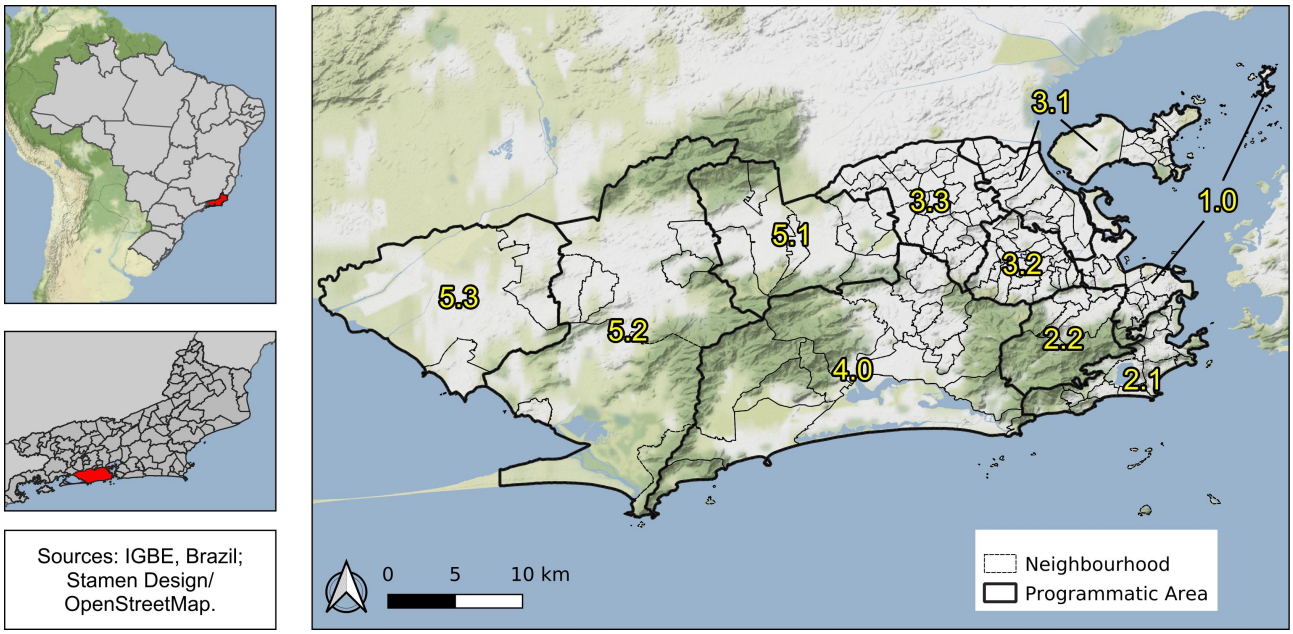

With three mountain massifs and 84 km of beaches, Rio has a diverse geography that is directly associated with the history of occupation and with socioeconomic disparities (Prefeitura do Rio de Janeiro, n.d.). The Downtown region is the historical, commercial and financial centre of the

medRxiv preprint doi: https://doi.org/10.1101/2020.06.08.20125757; this version posted June 9, 2020. The copyright holder for this preprint (which was not certified by peer review) is the author/funder, who has granted medRxiv a license to display the preprint in perpetuity. It is made available under a CC-BY 4.0 International license .

city, with many cultural establishments. The South region is the most popular tourist destination, with famous beaches and wealthy neighbourhoods, while in the North region there are very large slums ("favelas") and nearly 27% of the population, almost 2.4 million people, living in such communities (Cavallieri and Vial, 2012). The West region has more heterogeneous characteristics among its neighbourhoods, being the area 5.1 more densely populated, areas 5.2 and 5.3 less urbanized, and area 4.0 wealthier.

Data

Chikungunya cases

Data on chikungunya cases were obtained from the Notifiable Diseases Information System (SINAN) via the Rio de Janeiro Municipal Secretariat of Heath and are publicly available (Prefeitura do Rio de Janeiro and Secretaria Municipal de Saúde, 2016). Cases were geocoded to the neighbourhood of the patient's residence by the Municipal Secretariat of Health.

We analysed notified cases of chikungunya (confirmed by laboratory or clinical-epidemiological criteria) occurring in Rio de Janeiro municipality between January and December 2016, by week and neighbourhood.

Case definitions follow Ministry of Health protocols. A suspected case of chikungunya is defined as a patient with sudden fever of over 38.5°C and severe arthralgia or arthritis not explained by other conditions, and who either lives in endemic areas or has visited one up to two weeks before the onset of symptoms or has an epidemiological link with a confirmed case. A confirmed case is a suspected case with at least one positive specific laboratory test for CHIKV or confirmed by clinical-epidemiological criteria (Ministério da Saúde, 2017).

Socioeconomic data

Population and sociodevelopment index data by neighbourhood were obtained from the Instituto Pereira Passos (Prefeitura do Rio de Janeiro, 2019a, 2019b). The sociodevelopment index

medRxiv preprint doi: https://doi.org/10.1101/2020.06.08.20125757; this version posted June 9, 2020. The copyright holder for this preprint (which was not certified by peer review) is the author/funder, who has granted medRxiv a license to display the preprint in perpetuity. It is made available under a CC-BY 4.0 International license .

is based on eight indicators from the 2010 Demographic Census: 1) the percentage of domiciles with adequate water supply; 2) the percentage of domiciles with adequate sewage; 3) the percentage of domiciles with garbage collection; 4) the average number of toilets per resident; 5) the percentage of illiteracy among residents between 10 and 14 years old; 6) per capita income of the domiciles, expressed as minimum wages; 7) the percentage of domiciles with per capita income up to one minimum wage, and 8) the percentage of domiciles with per capita income greater than 5 minimum wage. The sociodevelopment index is calculated as the arithmetic average of the normalized indicators (each ranging from 0 to 1, being 0 the worst socioeconomic condition and 1, the best) (Prefeitura do Rio de Janeiro, 2019b).

Environment and temperature data

Land use data for the city of Rio de Janeiro were obtained from the Instituto Pereira Passos as a shapefile (Prefeitura do Rio de Janeiro, 2019c). We created the category “green area” by aggregating: agricultural areas, areas with swamps and shoals, areas with tree and shrub cover, and areas with woody-grass cover. Thereafter, we calculated the proportion of green area for each neighbourhood (Figure 4B).

Temperature information was obtained from 38 meteorological weather stations in Rio de Janeiro from 5 different meteorological and environmental institutes for 2016. The institutes are the Brazilian National Institute of Meteorology (INMET, n.d.), the Brazilian Airspace Control Department (DECEA, n.d.), the Rio de Janeiro State Environmental Institute (INEA, n.d.), the Rio de Janeiro Municipal Environmental Secretariat (SMAC, n.d.) and the Alerta Rio System (Prefeitura do Rio de Janeiro, n.d.), and its measurements are made according to the recommendations of the World Meteorological Organization (World Meteorological Organization, 2007). All institutes make their meteorological data publicly available, being that the frequency of measurements of the first four organizations is hourly, while the Alerta Rio System realizes measurements every 15 minutes.

medRxiv preprint doi: https://doi.org/10.1101/2020.06.08.20125757; this version posted June 9, 2020. The copyright holder for this preprint (which was not certified by peer review) is the author/funder, who has granted medRxiv a license to display the preprint in perpetuity. It is made available under a CC-BY 4.0 International license .

From the temperature measurements, we have computed the daily maximum, minimum and mean temperature, as well as we have evaluated the availability of the daily data in terms of missing measurements. The daily records that had more than 60% of missing measurements were excluded. We decided to use the minimum temperature as in tropical climates the minimum temperature acts as a limiting factor for the *Ae. aegypti* activity and population (Gomes et al., 2012; Lowe et al., 2017). We then obtained the minimum temperature for each week and station, and to obtain the minimum temperature by neighbourhood we applied universal kriging. Briefly, kriging is a method that uses a sample of data points to estimate the value of a given variable over a continuous space (Diggle and Ribeiro, 2007). First, we interpolated the minimum temperature to a grid with each unit measuring 500m x 500m. The grid with the meteorological weather stations is displayed in the Supplementary Material Figure 1. Then we obtained the minimum temperature of the neighbourhood by calculating the average of the minimum temperature of the grid units whose centroids were within the boundaries of the neighbourhood.

To process and organize the environmental data we used R version 3.6.1 (The R Foundation for Statistical Computing, 2020) and packages sf (Pebesma et al., 2019), geoR (Ripley et al., 2001) and tidyverse (Wickham and RStudio, 2017).

Statistical analysis

We used the Stan platform to fit spatial models, more specifically ICAR models, to a dataset consisting of neighbourhoods counts of chikungunya cases, exploring the effects of sociodevelopment index, green area proportion and minimum temperature. Let $Y_{i,t}$ be the counts of chikungunya cases at neighbourhood i = 1, 2, …, n = 160, and week t = 1, 2, … , T, where $Y_{i,t} \sim Poisson(\mu_{i,t})$ and we explored the following structures for $\mu_{i,t}$:

Model 0 $$\log(\mu_{i,t}) = \log(e_i) + \beta_0 + \phi_i$$

Model 1 $$\log(\mu_{i,t}) = \log(e_i) + \beta_0 + X'_i \beta_{k,t}$$

medRxiv preprint doi: https://doi.org/10.1101/2020.06.08.20125757; this version posted June 9, 2020. The copyright holder for this preprint (which was not certified by peer review) is the author/funder, who has granted medRxiv a license to display the preprint in perpetuity. It is made available under a CC-BY 4.0 International license .

Model 2 $$\log(\mu_{i,t}) = \log(e_i) + \beta_0 + X'_i \beta_{k,t} + \phi_i$$

Model 3 $$\log(\mu_{i,t}) = \log(e_i) + \beta_0 + U_{i,t} + \phi_i$$

$$U_{i,t} = \rho_i U_{i,t-1} + \zeta_i Temperature_{i,t}$$

Model 4 $$\log(\mu_{i,t}) = \log(e_i) + \beta_0 + X'_i \beta_{k,t} + U_{i,t} + \phi_i$$

$$U_{i,t} = \rho_i U_{i,t-1} + \zeta_i Temperature_{i,t}$$

The spatial effect is represented by ϕ, with each ϕ_i being normally distributed with a mean equal to the average of its neighbours (the neighbour relationship is written as $i \sim j$), and its variance decreases according to the number of neighbours d_i:

$$p(\phi_i | \phi_{i \sim j}) = N\left(\frac{\sum_{i \sim j} \phi_i}{d_i}, \frac{\sigma}{d_i}\right) \quad (1)$$

For all models e_i is the expected number of chikungunya cases at neighbourhood i, representing the number of cases that would have been observed if there were no differences in the incidence of cases across time and space:

$$e_i = \left(\frac{\sum_{i=1}^{n} \sum_{t=1}^{T} Y_{i,t}}{\sum_{i=1}^{n} population_i} population_i\right) / T \quad (2)$$

Model 0 includes only the intercept (β_0) and the spatial effect (ϕ). Model 1 represents the model with covariates without the spatial component, where X'_i represents a vector of k covariates and $\beta_{k,t}$ *is* the coefficient of covariate k in week t. We decided to consider time-varying coefficients for the covariates to explore if their effects in the number of cases vary as the epidemic progresses. The covariates included in the X'_i vector were sociodevelopment index and proportion of green area. The proportion of green area showed a skewed distribution, therefore this variable was transformed to the cubic root. We also fitted models including the population density, but the 90% credible interval of its coefficient included 0 for most weeks and the inclusion of this variable

medRxiv preprint doi: https://doi.org/10.1101/2020.06.08.20125757; this version posted June 9, 2020. The copyright holder for this preprint (which was not certified by peer review) is the author/funder, who has granted medRxiv a license to display the preprint in perpetuity. It is made available under a CC-BY 4.0 International license .

reduced the model fitting, hence, it was not considered in the final model. Model 2 includes both the covariates and the spatial component.

The temperature influences the number of cases over different times, therefore we estimate its effect using a transfer function ($U_{i,t}$) that considers that the temperature has an immediate effect (ζ_i) and that a proportion (ρ_i) of this effect propagates through future times. This proportion ρ_i is called memory effect and can be any value between 0 and 1. The main advantage of using a transfer function is that there is no need to specify the lag of the effect, the lag estimation is data-driven (Alves et al., 2010). To combine and visualize both effects of the temperature, we obtained the impulse response function of the temperature for each neighbourhood. This function expresses the effect of a 1 unit increase in the temperature of one week propagating in time (Alves et al., 2010). Model 3 is model 0 adding the transfer function $U_{i,t}$. The temperature was standardized. Finally, model 4 is model 3 adding the covariates.

The models were fitted under the Bayesian framework using the Stan platform (Carpenter et al., 2017) to run 4 chains of 10000 iterations each where the first 5000 were the warmup. We used visual inspection of the chains and R-hat statistic to check convergence (Gelman and Rubin, 1992; Stan Development Team, n.d.). Model selection was based on the Watanabe-Akaike information criterion (WAIC) (Watanabe, 2010). It is worth mentioning that we also fitted models that considered the reparametrization of the Besag-York-Mollié (BYM2) as proposed by Riebler et al., 2016, but the random component was over 90% spatial, and the unstructured effect was not statistically important in none of the neighbourhoods.

For the statistical analysis we used R version 3.6.1 (The R Foundation for Statistical Computing, 2020) and packages rstan (Guo et al., 2019) and loo (Vehtari et al., 2017). Maps and graphs were created using QGIS version 3.12 (QGIS Development Team, 2020) and ggplot2 version 3.2.0 (Wickham, 2016).

medRxiv preprint doi: https://doi.org/10.1101/2020.06.08.20125757; this version posted June 9, 2020. The copyright holder for this preprint (which was not certified by peer review) is the author/funder, who has granted medRxiv a license to display the preprint in perpetuity. It is made available under a CC-BY 4.0 International license .

Results

Between January and December 2016, 13,627 cases of chikungunya were notified in the city of Rio de Janeiro, corresponding to an incidence of 21.6 cases per 10,000 inhabitants. The number of cases peaked at week 17/2016, with 1118 chikungunya cases (Figure 3A). The cumulative number of cases by neighbourhood ranged from 0 (Grumari, area 4.0) to 721 (Realengo, area 5.1). The highest incidence was found in Catumbi (area 1.0), of 211.0 cases per 10,000 inhabitants (Figure 3B).

Figure 3. Notified chikungunya cases by week (A) and chikungunya cases cumulative incidence per 10,000 inhabitants by neighbourhood (B), January to December 2016, Rio de Janeiro city, Brazil.

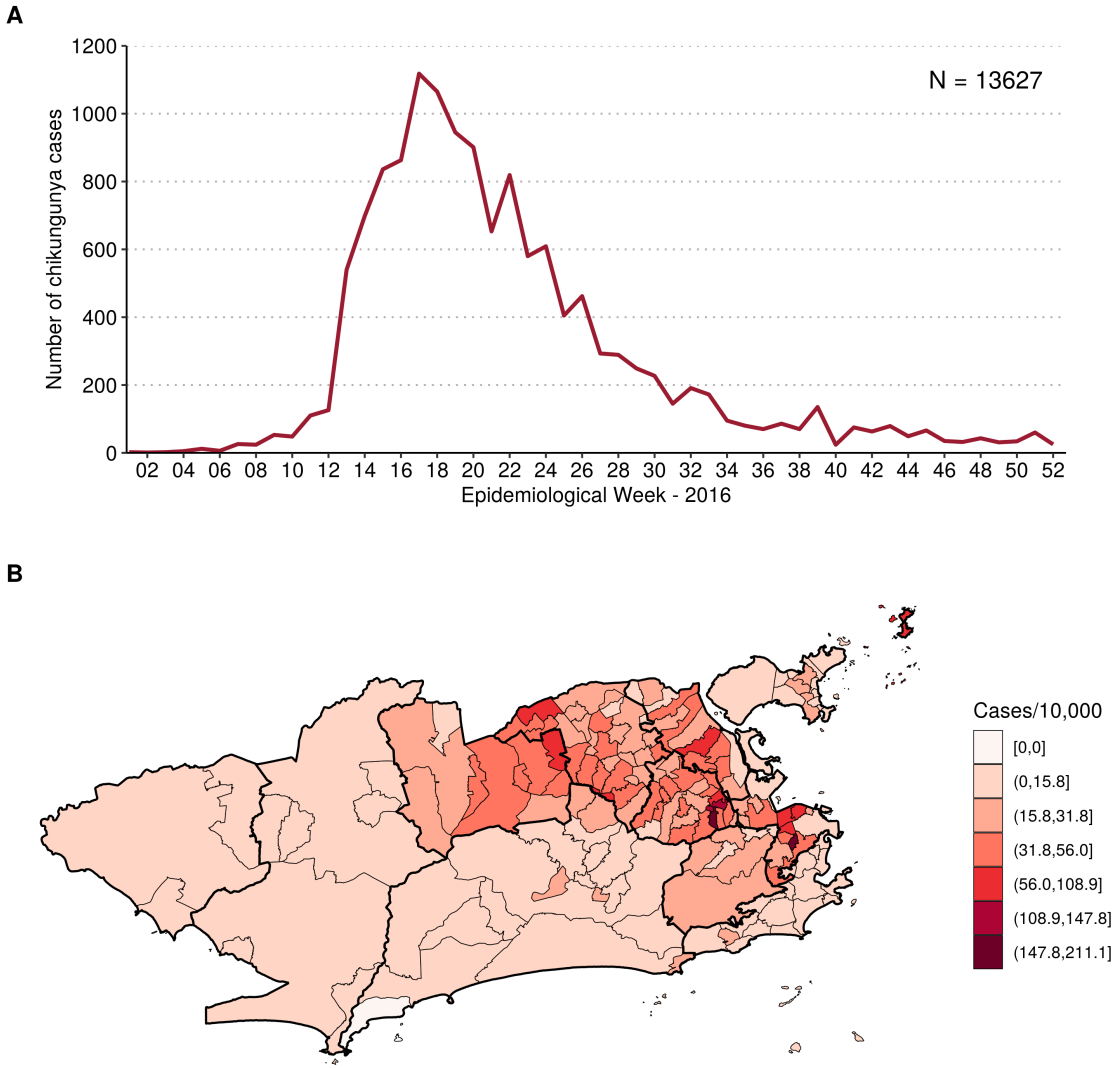

medRxiv preprint doi: https://doi.org/10.1101/2020.06.08.20125757; this version posted June 9, 2020. The copyright holder for this preprint (which was not certified by peer review) is the author/funder, who has granted medRxiv a license to display the preprint in perpetuity. It is made available under a CC-BY 4.0 International license .

The mean sociodevelopment index was 0.6080, ranging from 0.282 in Grumari (area 4.0) to 0.819 in Lagoa (area 2.1). Higher sociodevelopment indexes were observed in the areas 2.1 and 4.0 (Figure 4A). Fifteen neighbourhoods did not have any green area, mostly located in areas 1.0, 3.1, 3.2 and 3.3 (Figure 4B). Alto da Boa Vista (area 2.2) presented the highest percentage of green area, of 90.4%. The average minimum temperature was 19.9 °C, ranging from 10.7 °C in Campo dos Afonsos (area 5.1) to 26.1 °C in Cidade Nova (area 1.0). Neighbourhoods located in the east coastal region of Rio had higher temperatures on average (Figure 4C). Around week 17 the temperature decreased in the city, starting to increase again around week 35 (Figure 4D).

Figure 4. Sociodevelopment index in 2010 (A), percentage of green area coverage in 2015 (B), and minimum temperature (ºC) in 2016 average by neighbourhood (C) and boxplot by neighbourhood and week (D), Rio de Janeiro city, Brazil.

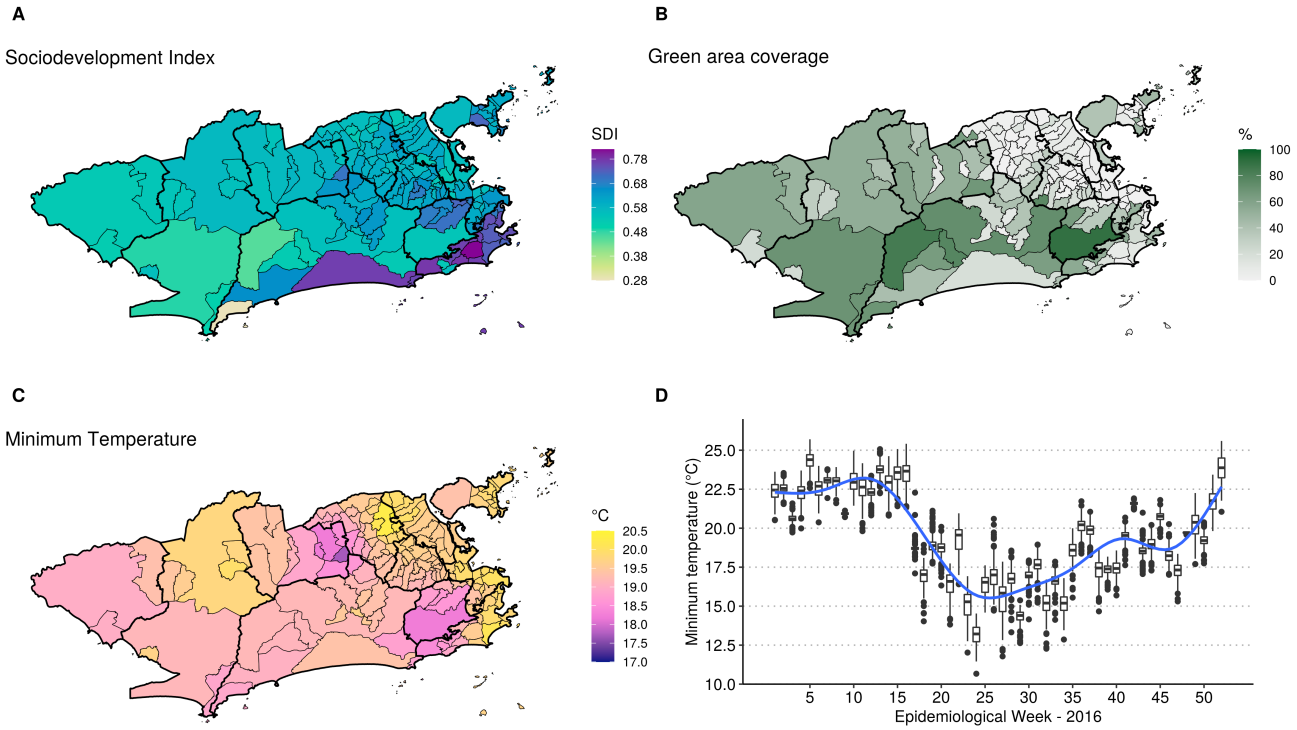

Due to the small numbers of chikungunya cases at the beginning of 2016, we decided to model the cases starting at week 9, when the number of cases in the city exceeded 50 for the first

medRxiv preprint doi: https://doi.org/10.1101/2020.06.08.20125757; this version posted June 9, 2020. The copyright holder for this preprint (which was not certified by peer review) is the author/funder, who has granted medRxiv a license to display the preprint in perpetuity. It is made available under a CC-BY 4.0 International license .

time. Model 4 had the best fit (WAIC = 17934.8) followed by Model 2 (WAIC = 19656.6), Model 3 (WAIC = 21262.1), Model 1 (WAIC = 26418.3) and finally Model 0 (WAIC = 34114.6).

The posterior summary of the time-varying coefficients for sociodevelopment index and proportion of green area for each model are presented in Figure 5. The sociodevelopment index consistently presented a protective effect, inversely associated with the epidemic curve. As the number of cases increased, the protective effect of the sociodevelopment index decreased, remaining almost constant during the peak of the epidemic, and increased again once the number of cases started decreasing. Actually, for Model 4 the effect of this variable was null during the peak of the epidemic (around week 17). The proportion of green area presented a protective effect in Model 1. However, once we included the spatial component in the model, its effect moved towards the null.

Figure 5. Time-varying coefficients (in the log scale) for sociodevelopment index (SDI) and green area proportion for spatial models for chikungunya cases from weeks 9 to 52 2016, Rio de Janeiro city, Brazil.

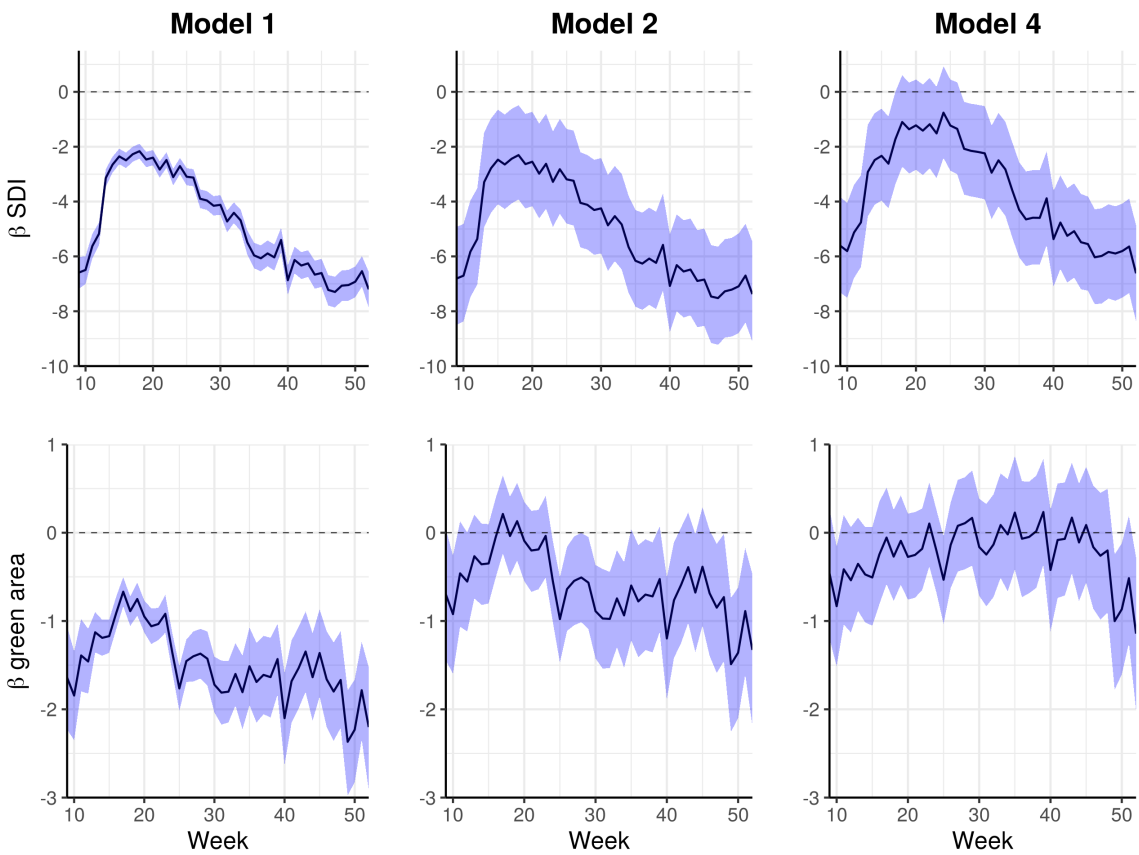

medRxiv preprint doi: https://doi.org/10.1101/2020.06.08.20125757; this version posted June 9, 2020. The copyright holder for this preprint (which was not certified by peer review) is the author/funder, who has granted medRxiv a license to display the preprint in perpetuity. It is made available under a CC-BY 4.0 International license .

The inclusion of the covariates and the transfer function in Model 4 decreased the spatial effects compared to Model 0 in 102 of the 160 neighbourhoods (Supplementary Material Figure 2). Overall, all models presented similar spatial effects structure, with a clear trend of positive spatial effects in areas where the epidemic was concentrated (areas 1.0, 2.2, the mainland part of 3.1, 3.2, 3.3 and 5.1) and negative spatial effects in less affected areas (Figure 6).

Figure 6. Chikungunya cases spatial effects (in the log scale) for Model 4, weeks 9 to 52 2016, Rio de Janeiro city, Brazil.

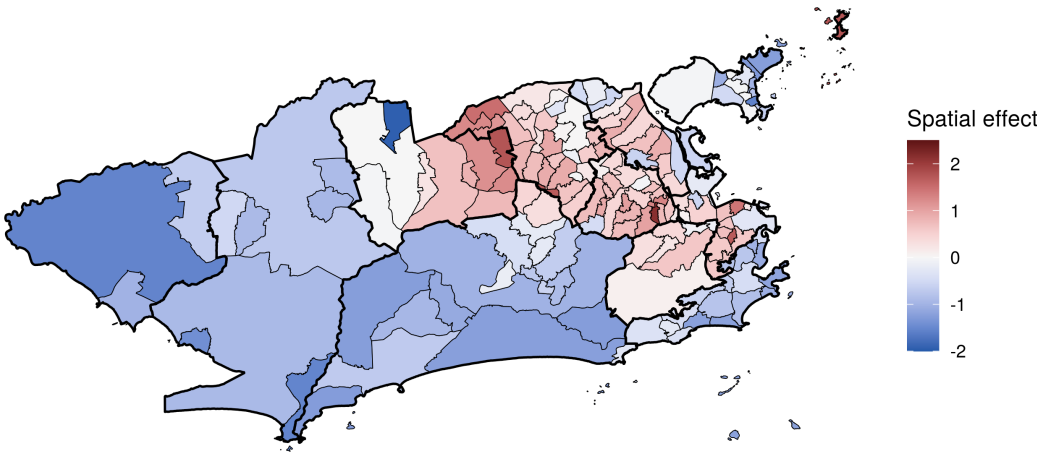

The posterior distributions of the instantaneous and memory effects of the minimum temperature are displayed in Figure 7. For most neighbourhoods (113/160, or 70.6%) the instantaneous effect of the temperature increased the risk of chikungunya cases (Figure 7A). The temperature instantaneous effect, however, was in general small, reaching its maximum in Catumbi (area 1.0), where the temperature relative risk was 2.28 (90%CI 2.07-2.53). The memory effect represents the proportion of the instantaneous effect that propagates in time. Therefore, for neighbourhoods where the temperature effect was null, the memory effect is irrelevant.

medRxiv preprint doi: https://doi.org/10.1101/2020.06.08.20125757; this version posted June 9, 2020. The copyright holder for this preprint (which was not certified by peer review) is the author/funder, who has granted medRxiv a license to display the preprint in perpetuity. It is made available under a CC-BY 4.0 International license .

Figure 7. Minimum temperature instantaneous effect (in the same week) (A) and memory effect (B) on chikungunya cases (in the log scale) by neighbourhood, mean and 90% credible interval, weeks 9 to 52 2016, Rio de Janeiro city, Brazil.

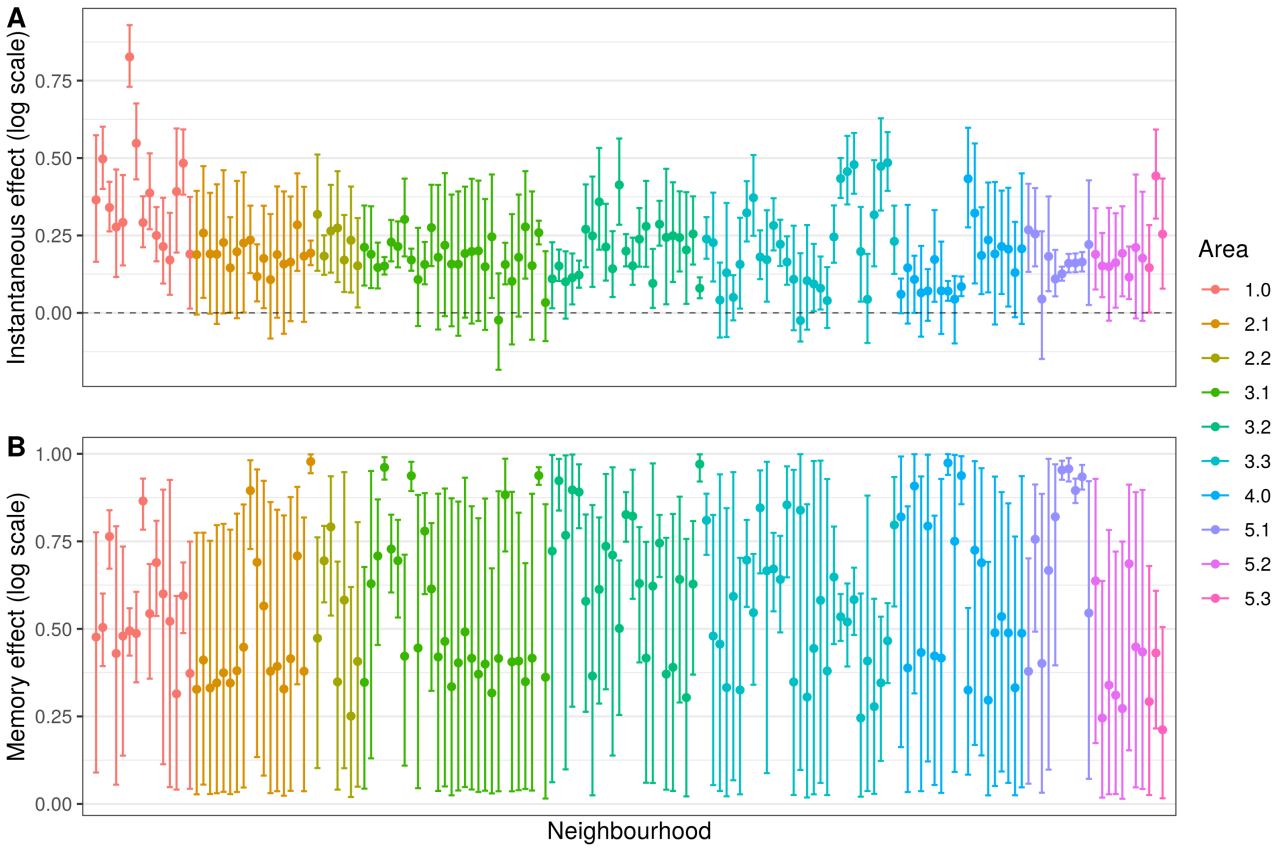

When we combine the instantaneous and the memory effects in the impulse response function, we observed three patterns, exemplified with 9 selected neighbourhoods in Figure 8: null effect (Figure 8 first row), rapid decay of the effect (second row), and slow decay of the effect (third row). The impulse response functions for all neighbourhoods are available in the Supplementary Material Figure 3.

The impulse response function is represented in time and space in Video 1. The first frame represents the mean temperature instantaneous relative risk, the impulse, and the following frames represent the propagation of this impulse on subsequent weeks. When the temperature relative risk is null (90% credible interval includes the 1), the neighbourhood is depicted blank. The strong

medRxiv preprint doi: https://doi.org/10.1101/2020.06.08.20125757; this version posted June 9, 2020. The copyright holder for this preprint (which was not certified by peer review) is the author/funder, who has granted medRxiv a license to display the preprint in perpetuity. It is made available under a CC-BY 4.0 International license .

memory effect in some neighbourhoods (Figure 7B) is observed in Video 1 by the persistence of the temperature effect for several weeks after the impulse, although such effect declines to values very close to 1. These neighbourhoods were concentrated in areas 1.0, 2.2, mainland 3.1, 3.2, 3.3 and 5.1.

Figure 8. Impulse response function of the minimum temperature effect on chikungunya cases over time, posterior mean and 90% credible interval, in selected neighbourhoods, Rio de Janeiro city, Brazil.

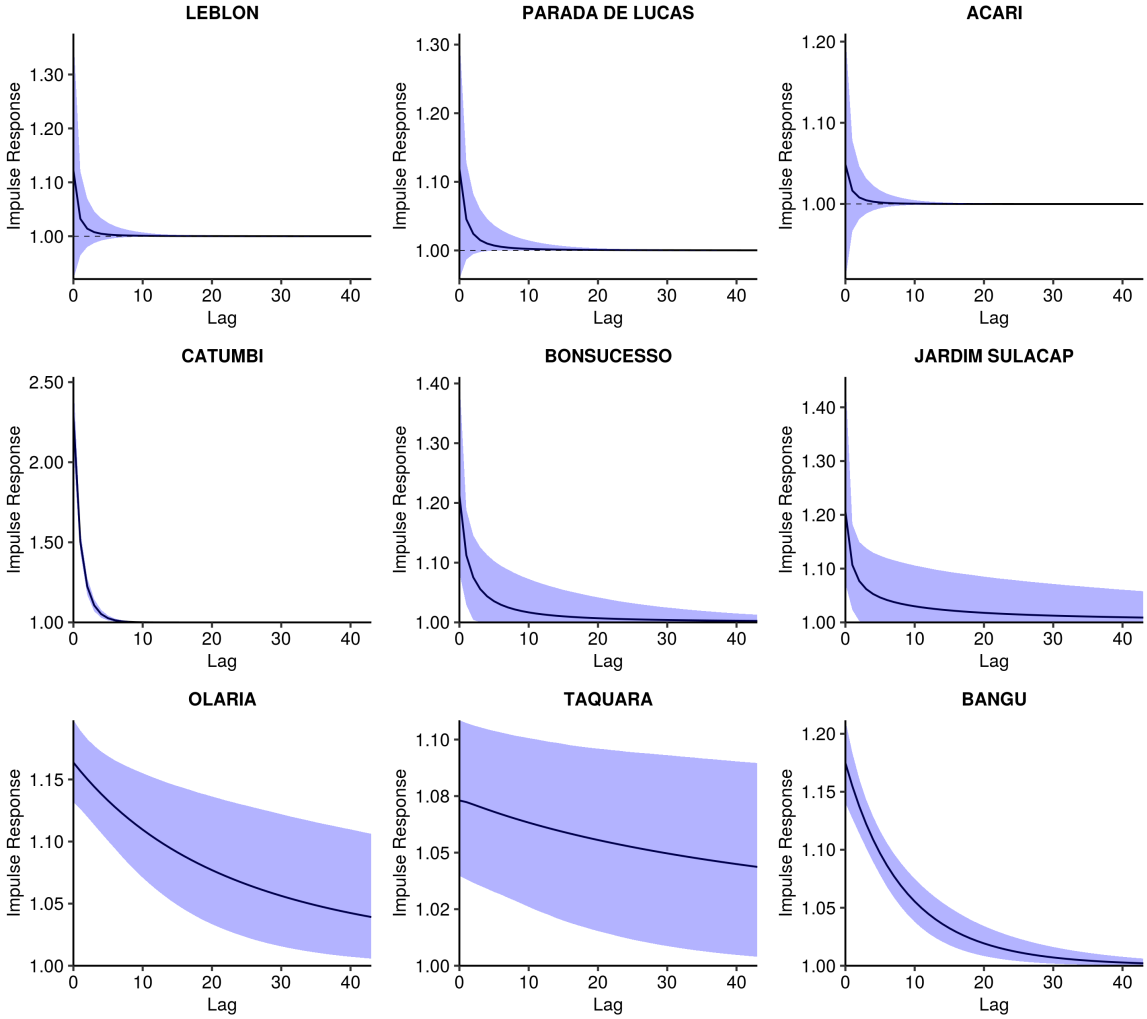

Video 1. Minimum temperature instantaneous effect on chikungunya cases and its propagation in time by neighbourhood, Rio de Janeiro city, Brazil.

medRxiv preprint doi: https://doi.org/10.1101/2020.06.08.20125757; this version posted June 9, 2020. The copyright holder for this preprint (which was not certified by peer review) is the author/funder, who has granted medRxiv a license to display the preprint in perpetuity. It is made available under a CC-BY 4.0 International license .

The estimated relative risk increased rapidly in the first weeks, peaking at week 17 and then decaying progressively (Video 2 and Figure 9). The decrease in the relative risk coincided with the decrease in the minimum temperature in the city (Figure 4D). High relative risks for chikungunya were mostly observed in areas 1.0, 2.2, 3.1, 3.2, 3.3 and 5.1. The neighbourhoods of the remaining areas presented relative risks below 1 for almost the entire study period. The relative risks with the credible interval are available in the Supplementary Material Figure 4.

Figure 9. Posterior chikungunya relative risk by neighbourhood in selected weeks, Rio de Janeiro city, Brazil.

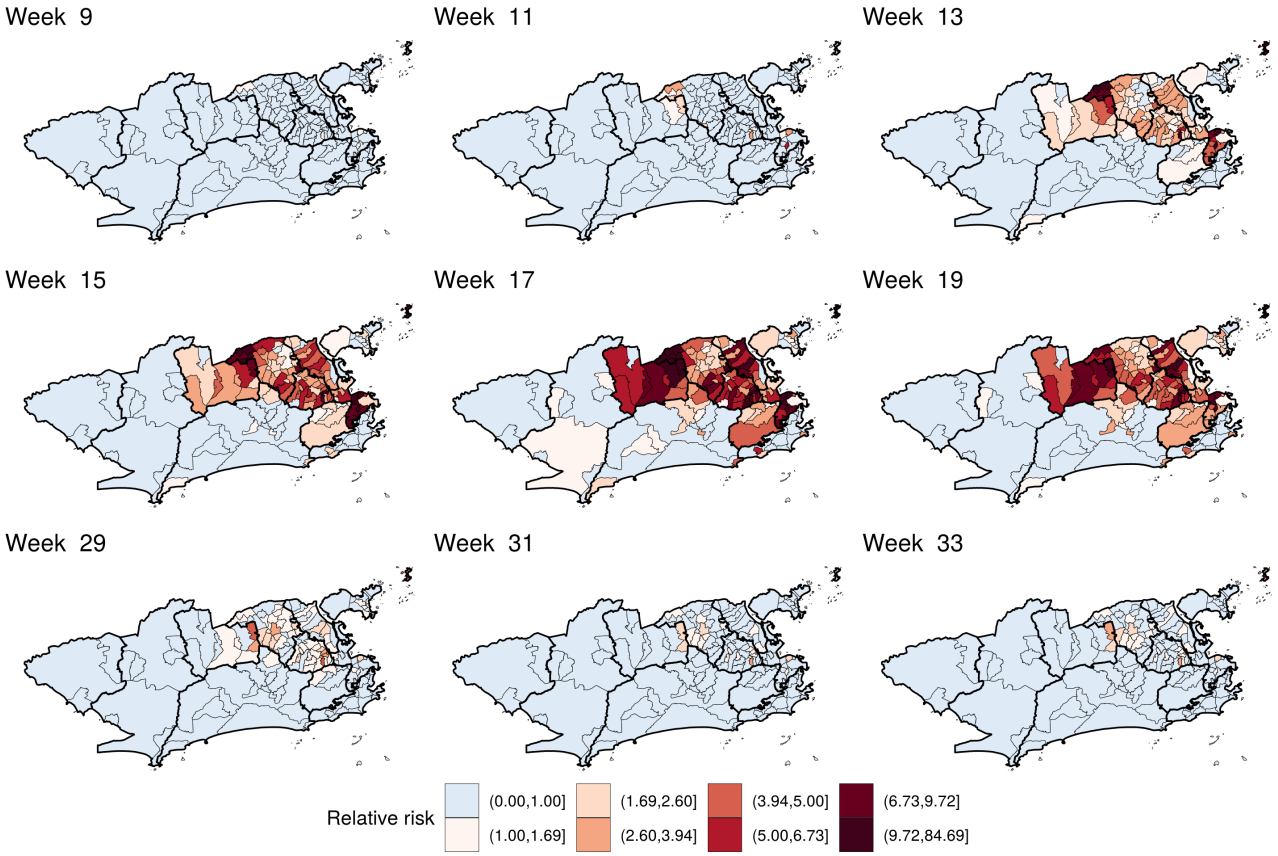

Video 2. Posterior chikungunya relative risk by neighbourhood, weeks 9 to 52 2016, Rio de Janeiro city, Brazil.

medRxiv preprint doi: https://doi.org/10.1101/2020.06.08.20125757; this version posted June 9, 2020. The copyright holder for this preprint (which was not certified by peer review) is the author/funder, who has granted medRxiv a license to display the preprint in perpetuity. It is made available under a CC-BY 4.0 International license .

Discussion

In this study, we present spatio-temporal models fitted to estimate the distribution of the first chikungunya epidemic in Rio de Janeiro city using as covariates factors that are indirectly related to the main necessary elements of an arboviral epidemic (Figure 1). The sociodevelopment index and the proportion of green area were included in the model with time-varying coefficients, which allowed us to explore how the effects of these factors changed with the progression of the epidemic. The temperature was included in the model using a transfer function, allowing for a memory effect that propagates in time, in addition to the instantaneous effect. To our knowledge, this is the first time a transfer function is applied for temperature when modelling arboviral diseases.

We consistently found the sociodevelopment index inversely associated with the risk of chikungunya in all models (Figure 5A). This index is composed of sanitary conditions indicators, among others, and poor sanitary conditions are known to favour the reproduction of the *Ae. aegypti* mosquitoes. The association of low socioeconomic locations with increased risk of chikungunya was also found in a study in French Guiana (Bonifay et al., 2017) and in a study in Barraquilla, a Colombian city (McHale et al., 2019). Our results indicate that poor neighbourhoods were the first ones to be affected by the chikungunya epidemic. In the event that another new arbovirus enters the city, this could also be the case, highlighting the importance of vector control activities in these locations.

When the spatial dependency was not considered (Model 1), the green area proportion had a negative association with the number of chikungunya cases (Figure 5). Such association was observed for dengue in São Paulo, where low vegetation cover areas presented higher dengue incidence rates (Teixeira and Cruz, 2011). However, with the inclusion of the spatial component (Models 2 and 4) the effect of the green area proportion moved towards null. This is possible due to spatial confounding, which happens when covariates that are spatially smooth are collinear with spatial random effects (Clayton et al., 1993).

medRxiv preprint doi: https://doi.org/10.1101/2020.06.08.20125757; this version posted June 9, 2020. The copyright holder for this preprint (which was not certified by peer review) is the author/funder, who has granted medRxiv a license to display the preprint in perpetuity. It is made available under a CC-BY 4.0 International license .

The temperature was important for most neighbourhoods, increasing the risk of chikungunya. In our models, we assumed that the temperature has an instantaneous effect and that a proportion of this effect propagates in time (the memory effect). The instantaneous one represents the effect of the temperature on the activity of the mosquito and human behaviour. The biting rate of the *Ae. aegypti* increases with the temperature until around 35 °C (Mordecai et al., 2017), while people become more exposed to mosquitoes in warm temperatures. The temperature also accelerates the extrinsic incubation period of the virus in the mosquito, and transmission was estimated to peak around 28.5 °C (Mordecai et al., 2017). On the other hand, the temperature effect on the population of mosquitoes by increasing fecundity, egg-to-adult-survival, development rate and lifespan, is not only on the same week but also accumulates in time, which is captured by the memory effect. It is important to note that for each of these elements of the mosquito ecology the temperature effect is not linear, but reaches a peak and then starts decreasing. For example, the biting rate decreases in temperatures above 35 °C (Mordecai et al., 2017).

Interestingly, the CHIKV epidemic in Rio de Janeiro in 2016 did not reach the whole city, with high-risk areas mostly concentrated in the North and Downtown regions. The decrease in the number of cases coincided with the decrease in the minimum temperature, around week 17 (Figures 3A and 4D). These two observations combined suggest that the epidemic was interrupted not because of the depletion of the susceptible human population, but because the decrease in the temperature caused a reduction in the transmission in such a way that the epidemic was not sustained. It is important to note that although the number of cases diminished substantially, there were still chikungunya cases being reported until the end of the year. Rio de Janeiro is a tropical city and the minimum temperature rarely is below the minimum temperature needed for transmission to occur, of 13.5 °C (Mordecai et al., 2017). A previous study conducted in the city showed that the *Ae. aegypti* population varies seasonally, but the mosquito is present all over the

medRxiv preprint doi: https://doi.org/10.1101/2020.06.08.20125757; this version posted June 9, 2020. The copyright holder for this preprint (which was not certified by peer review) is the author/funder, who has granted medRxiv a license to display the preprint in perpetuity. It is made available under a CC-BY 4.0 International license .

year (Honório et al., 2009b). This could explain the long persistence of the temperature effect in time in some neighbourhoods (Video 1).

Spatial models are important and useful to identify high-risk areas for diseases. The application of such models considering intra-urban scenarios is still growing for arboviral diseases. Our study identified high-risk neighbourhoods for chikungunya first epidemic in Rio de Janeiro city, which concentrated mostly in the North and Downtown regions (Figure 9 and Video 2). Such regions were already identified as high-risk locations for dengue (Xavier et al., 2017). In our previous study, neighbourhoods from these regions were more likely to constitute simultaneous clusters for dengue, Zika and chikungunya (Freitas et al., 2019). These regions have a combination of factors that favours the *Ae. aegypti* ecology and the transmission of arboviral diseases: low vegetation, low socioeconomic status and increased temperature (Figure 4). Vector control activities should be prioritized and intensified in the identified high-risk areas, as they appear to be the first ones affected by the epidemic. Also, the long-term persistence of the temperature effect (Video 1) and of a small number of cases even after the decline of the epidemic indicate that the mosquito continues to circulate and transmit the disease throughout the year, meaning interventions should be continuous in these locations.

Our study has some limitations. As for any study using secondary data on arboviral diseases, there is an uncertainty on the diagnosis of the reported cases as well as underreporting. It is important to consider that in the same year the city was also experiencing dengue and Zika epidemics (Freitas et al., 2019). Because of the association between Zika and severe congenital manifestations, the disease awareness around Zika may have improved the reporting rates (Lowe et al., 2018a). However, the simultaneous occurrence of three arbovirus epidemics may have impaired the differential diagnosis, as they cause similar symptoms. We analysed the data aggregated at the neighbourhood level as the data are more reliable at this spatial unit, but smaller areas inside the same neighbourhood can present different socioeconomic and environmental characteristics. Finer

medRxiv preprint doi: https://doi.org/10.1101/2020.06.08.20125757; this version posted June 9, 2020. The copyright holder for this preprint (which was not certified by peer review) is the author/funder, who has granted medRxiv a license to display the preprint in perpetuity. It is made available under a CC-BY 4.0 International license .

scales such as census tracts should be considered in future studies. Finally, an important limitation is the assumption that the chikungunya risk is related to the neighbourhood of residence, while some people may get infected in other locations.

The model here presented has the potential to be applied to other cities and other urban arboviral diseases. However, this may depend on the climate of the city. If the temperature presents a wide range of variation and reaches values that can either boost or impair transmission, a time-varying instantaneous effect for the temperature should be explored (Alves et al., 2010). Mosquito population information is expensive to collect and often unreliable. Therefore not depending on such data is a strength of our model. By using temperature, socioeconomic and green area data as proxies of the key elements of arboviruses transmission, our model contributed to better understand the spatio-temporal dynamics of the first chikungunya epidemic in a tropical metropolitan city.

Acknowledgements

The authors would like to thank the Municipal Secretariat of Health for providing the data on reported cases, and the meteorological and environmental institutes – INMET, DECEA, INEA, SMAC and Alerta Rio, for making their meteorological data publicly available.

Competing interests

We declare we have no competing interests.

Funding

This study was financed in part by the Coordenação de Aperfeiçoamento de Pessoal de Nível Superior - Brasil (CAPES) - Finance Code 001, to LPF. LPF received funds from the Emerging Leaders in the Americas Program (ELAP), Government of Canada. AMS acknowledges the support of the Natural Sciences and Engineering Research Council (NSERC) of Canada (RGPIN-2017-

medRxiv preprint doi: https://doi.org/10.1101/2020.06.08.20125757; this version posted June 9, 2020. The copyright holder for this preprint (which was not certified by peer review) is the author/funder, who has granted medRxiv a license to display the preprint in perpetuity. It is made available under a CC-BY 4.0 International license .

04999). MSC received grants from Fundação Carlos Chagas Filho de Amparo à Pesquisa do Estado do Rio de Janeiro (FAPERJ, grant nº E_26/201.356/2014) and support from Conselho Nacional de Desenvolvimento Científico e Tecnológico (CNPq, grant nº 304101/2017-6). The funders did not influence the content of this manuscript nor the decision to submit it for publication.

References

Alves MB, Gamerman D, Ferreira MA. 2010. Transfer functions in dynamic generalized linear models. *Statistical Modelling: An International Journal* **10**:03–40. doi:10.1177/1471082X0801000102

Besag J. 1974. Spatial Interaction and the Statistical Analysis of Lattice Systems. *Journal of the Royal Statistical Society Series B (Methodological)* **36**:192–236.

Bonifay T, Douine M, Bonnefoy C, Hurpeau B, Nacher M, Djossou F, Epelboin L. 2017. Poverty and Arbovirus Outbreaks: When Chikungunya Virus Hits More Precarious Populations Than Dengue Virus in French Guiana. *Open Forum Infectious Diseases* **4**. doi:10.1093/ofid/ofx247

Carpenter B, Gelman A, Hoffman MD, Lee D, Goodrich B, Betancourt M, Brubaker M, Guo J, Li P, Riddell A. 2017. *Stan* : A Probabilistic Programming Language. *Journal of Statistical Software* **76**. doi:10.18637/jss.v076.i01

Carvalho MS, Freitas LP, Cruz OG, Brasil P, Bastos LS. 2020. Association of past dengue fever epidemics with the risk of Zika microcephaly at the population level in Brazil. *Scientific Reports* **10**. doi:10.1038/s41598-020-58407-7

Carvalho MS, Honorio NA, Garcia LMT, Carvalho LC de S. 2017. Aedes ægypti control in urban areas: A systemic approach to a complex dynamic. *PLOS Neglected Tropical Diseases* **11**:e0005632. doi:10.1371/journal.pntd.0005632

medRxiv preprint doi: https://doi.org/10.1101/2020.06.08.20125757; this version posted June 9, 2020. The copyright holder for this preprint (which was not certified by peer review) is the author/funder, who has granted medRxiv a license to display the preprint in perpetuity. It is made available under a CC-BY 4.0 International license .

Cavallieri F, Vial A. 2012. Favelas na cidade do Rio de Janeiro: o quadro populacional com base no Censo 2010 (No. 20120501), Coleção Estudos Cariocas. Rio de Janeiro, RJ: Instituto Pereira Passos.

Clayton DG, Bernardinelli L, Montomoli C. 1993. Spatial Correlation in Ecological Analysis. *International Journal of Epidemiology* **22**:1193–1202. doi:10.1093/ije/22.6.1193

de Souza T, Ribeiro E, Corrêa V, Damasco P, Santos C, de Bruycker-Nogueira F, Chouin-Carneiro T, Faria N, Nunes P, Heringer M, Lima M, Badolato-Corrêa J, Cipitelli M, Azeredo E, Nogueira R, dos Santos F. 2018. Following in the Footsteps of the Chikungunya Virus in Brazil: The First Autochthonous Cases in Amapá in 2014 and Its Emergence in Rio de Janeiro during 2016. *Viruses* **10**:623. doi:10.3390/v10110623

DECEA. n.d. REDEMET - Painel de consulta. *Rede de Meteorologia do Comando da Aeronáutica*. https://www.redemet.aer.mil.br/?i=produtos&p=consulta-de-mensagens-opmet

Diggle P, Ribeiro PJ. 2007. Model-based Geostatistics, Springer Series in Statistics. New York: Springer-Verlag. doi:10.1007/978-0-387-48536-2

Freitas LP, Cruz OG, Lowe R, Sá Carvalho M. 2019. Space-time dynamics of a triple epidemic: dengue, chikungunya and Zika clusters in the city of Rio de Janeiro. *Proceedings of the Royal Society B: Biological Sciences* **286**:20191867. doi:10.1098/rspb.2019.1867

Gelman A, Rubin DB. 1992. Inference from Iterative Simulation Using Multiple Sequences. *Statistical Science* **7**:457–472. doi:10.1214/ss/1177011136

Gomes AF, Nobre AA, Cruz OG. 2012. Temporal analysis of the relationship between dengue and meteorological variables in the city of Rio de Janeiro, Brazil, 2001-2009. *Cadernos de Saúde Pública* **28**:2189–2197. doi:10.1590/S0102-311X2012001100018

Guo J, Gabry J, Goodrich B, Lee D, Sakrejda K, Martin M, University T of C, Sklyar (R/cxxfunplus.R) O, Team (R/pairs.R TRC, R/dynGet.R), Oehlschlaegel-Akiyoshi (R/pairs.R) J. 2019. rstan: R Interface to Stan.

medRxiv preprint doi: https://doi.org/10.1101/2020.06.08.20125757; this version posted June 9, 2020. The copyright holder for this preprint (which was not certified by peer review) is the author/funder, who has granted medRxiv a license to display the preprint in perpetuity. It is made available under a CC-BY 4.0 International license .

Honório NA, Castro MG, Barros FSM de, Magalhães M de AFM, Sabroza PC. 2009a. The spatial distribution of Aedes aegypti and Aedes albopictus in a transition zone, Rio de Janeiro, Brazil. *Cadernos de Saúde Pública* **25**:1203–1214. doi:10.1590/S0102-311X2009000600003

Honório NA, Codeço CT, Alves FC, Magalhães M de AFM, Lourenço-de-Oliveira R. 2009b. Temporal Distribution of *Aedes aegypti* in Different Districts of Rio De Janeiro, Brazil, Measured by Two Types of Traps. *Journal of Medical Entomology* **46**:1001–1014. doi:10.1603/033.046.0505

Honório NA, Nogueira RMR, Codeço CT, Carvalho MS, Cruz OG, Magalhães M de AFM, de Araújo JMG, de Araújo ESM, Gomes MQ, Pinheiro LS, da Silva Pinel C, Lourenço-de-Oliveira R. 2009c. Spatial Evaluation and Modeling of Dengue Seroprevalence and Vector Density in Rio de Janeiro, Brazil. *PLoS Neglected Tropical Diseases* **3**:e545. doi:10.1371/journal.pntd.0000545

INEA. n.d. Dados do Monitoramento da Qualidade do Ar e Meteorologia. *Instituto Estadual do Ambiente Rio de Janeiro*. http://200.20.53.25/qualiar/home/index

INMET. n.d. Estações Automáticas. *INMET - Instituto Nacional de Meteorologia*. http://www.inmet.gov.br/portal/index.php?r=estacoes/estacoesAutomaticas

Kuno G. 1995. Review of the Factors Modulating Dengue Transmission. *Epidemiologic Reviews* **17**:321–335. doi:10.1093/oxfordjournals.epirev.a036196

Lowe R, Bailey TC, Stephenson DB, Graham RJ, Coelho CAS, Sá Carvalho M, Barcellos C. 2011. Spatio-temporal modelling of climate-sensitive disease risk: Towards an early warning system for dengue in Brazil. *Computers & Geosciences* **37**:371–381. doi:10.1016/j.cageo.2010.01.008

medRxiv preprint doi: https://doi.org/10.1101/2020.06.08.20125757; this version posted June 9, 2020. The copyright holder for this preprint (which was not certified by peer review) is the author/funder, who has granted medRxiv a license to display the preprint in perpetuity. It is made available under a CC-BY 4.0 International license .

Lowe R, Barcellos C, Brasil P, Cruz OG, Honório NA, Kuper H, Carvalho MS. 2018a. The Zika Virus Epidemic in Brazil: From Discovery to Future Implications. *International Journal of Environmental Research and Public Health* **15**:96. doi:10.3390/ijerph15010096

Lowe R, Gasparrini A, Van Meerbeeck CJ, Lippi CA, Mahon R, Trotman AR, Rollock L, Hinds AQJ, Ryan SJ, Stewart-Ibarra AM. 2018b. Nonlinear and delayed impacts of climate on dengue risk in Barbados: A modelling study. *PLOS Medicine* **15**:e1002613. doi:10.1371/journal.pmed.1002613

Lowe R, Stewart-Ibarra AM, Petrova D, García-Díez M, Borbor-Cordova MJ, Mejía R, Regato M, Rodó X. 2017. Climate services for health: predicting the evolution of the 2016 dengue season in Machala, Ecuador. *The Lancet Planetary Health* **1**:e142–e151. doi:10.1016/S2542-5196(17)30064-5

Martínez-Bello D, López-Quílez A, Torres Prieto A. 2018. Spatio-Temporal Modeling of Zika and Dengue Infections within Colombia. *International Journal of Environmental Research and Public Health* **15**:1376. doi:10.3390/ijerph15071376

Martínez-Bello DA, López-Quílez A, Torres Prieto A. 2017. Relative risk estimation of dengue disease at small spatial scale. *International Journal of Health Geographics* **16**. doi:10.1186/s12942-017-0104-x

McHale TC, Romero-Vivas CM, Fronterre C, Arango-Padilla P, Waterlow NR, Nix CD, Falconar AK, Cano J. 2019. Spatiotemporal Heterogeneity in the Distribution of Chikungunya and Zika Virus Case Incidences during their 2014 to 2016 Epidemics in Barranquilla, Colombia. *International Journal of Environmental Research and Public Health* **16**:1759. doi:10.3390/ijerph16101759

Ministério da Saúde. 2017. Chikungunya: manejo clínico. Brasília, DF.

Mordecai EA, Cohen JM, Evans MV, Gudapati P, Johnson LR, Lippi CA, Miazgowicz K, Murdock CC, Rohr JR, Ryan SJ, Savage V, Shocket MS, Stewart Ibarra A, Thomas MB, Weikel DP.

medRxiv preprint doi: https://doi.org/10.1101/2020.06.08.20125757; this version posted June 9, 2020. The copyright holder for this preprint (which was not certified by peer review) is the author/funder, who has granted medRxiv a license to display the preprint in perpetuity. It is made available under a CC-BY 4.0 International license .

2017. Detecting the impact of temperature on transmission of Zika, dengue, and chikungunya using mechanistic models. *PLOS Neglected Tropical Diseases* **11**:e0005568. doi:10.1371/journal.pntd.0005568

Morris M, Wheeler-Martin K, Simpson D, Mooney SJ, Gelman A, DiMaggio C. 2019. Bayesian hierarchical spatial models: Implementing the Besag York Mollié model in stan. *Spatial and Spatio-temporal Epidemiology* **31**:100301. doi:10.1016/j.sste.2019.100301

Nogueira RMR, Miagostovich MP, Schatzmayr HG, Santos FB dos, Araújo ESM de, Filippis AMB de, Souza RV de, Zagne SMO, Nicolai C, Baran M, Teixeira Filho G. 1999. Dengue in the State of Rio de Janeiro, Brazil, 1986-1998. *Memórias do Instituto Oswaldo Cruz* **94**:297–304. doi:10.1590/S0074-02761999000300004

Pebesma E, Bivand R, Racine E, Sumner M, Cook I, Keitt T, Lovelace R, Wickham H, Ooms J, Müller K, Pedersen TL. 2019. sf: Simple Features for R.

Prefeitura do Rio de Janeiro. 2019a. População residente, por idade e por grupos de idade, segundo as Áreas de Planejamento (AP), Regiões Administrativas (RA) e Bairros em 2000/2010. *Data Rio*. http://www.data.rio/datasets/e68e54eaa6bb484dbb40828acf2b3e7e

Prefeitura do Rio de Janeiro. 2019b. Índice de Desenvolvimento Social (IDS) por Áreas de Planejamento (AP), Regiões de Planejamento (RP), Regiões Administrativas (RA), Bairros e Favelas do Município do Rio de Janeiro - 2010. *Data Rio*. http://www.data.rio/datasets/fa85ddc76a524380ad7fc60e3006ee97

Prefeitura do Rio de Janeiro. 2019c. Uso do Solo 2015. *Data Rio*. http://www.data.rio/datasets/e74a94ac95d440d19b3e18c23bc485de_6

Prefeitura do Rio de Janeiro. n.d. Rio em Síntese. *Data Rio*. http://www.data.rio/pages/rio-em-sntese-2

Prefeitura do Rio de Janeiro. n.d. Dados Meteorológicos. *SIstema Alerta Rio*. http://alertario.rio.rj.gov.br/download/dados-meteorologicos/

medRxiv preprint doi: https://doi.org/10.1101/2020.06.08.20125757; this version posted June 9, 2020. The copyright holder for this preprint (which was not certified by peer review) is the author/funder, who has granted medRxiv a license to display the preprint in perpetuity. It is made available under a CC-BY 4.0 International license .

Prefeitura do Rio de Janeiro, Secretaria Municipal de Saúde. 2016. Número de Casos de Chikungunya por Semana Epidemiológica, Áreas de Planejamento, Regiões Administrativas e Bairros - Município do Rio de Janeiro, 2016. http://www.rio.rj.gov.br/dlstatic/10112/7612791/4213019/CHIKVSE2016.pdf

QGIS Development Team. 2020. QGIS Geographic Information System. Open Source Geospatial Foundation Project.

Randolph SE, Rogers DJ. 2010. The arrival, establishment and spread of exotic diseases: patterns and predictions. *Nature Reviews Microbiology* **8**:361–371. doi:10.1038/nrmicro2336

Riebler A, Sørbye SH, Simpson D, Rue H. 2016. An intuitive Bayesian spatial model for disease mapping that accounts for scaling: *Statistical Methods in Medical Research*. doi:10.1177/0962280216660421

Ripley BD, Ribeiro PJ, Diggle PJ. 2001. geoR: A Package for Geostatistical Analysis.

Rosa-Freitas MG, Tsouris P, Reis IC, Magalhães M de AFM, Nascimento TFS, Honório NA. 2010. Dengue land cover heterogeneity in Rio de Janeiro. *Oecologia Australis* **14**:641–667. doi:10.4257/oeco.2010.1403.04

Santos JPC dos, Honório NA, Nobre AA. 2019. Definition of persistent areas with increased dengue risk by detecting clusters in populations with differing mobility and immunity in Rio de Janeiro, Brazil. *Cadernos de Saúde Pública* **35**. doi:10.1590/0102-311x00248118

SMAC. n.d. Dados horários do monitoramento da qualidade do ar - MonitorAr. *Data Rio*. http://www.data.rio/datasets/dados-hor%C3%A1rios-do-monitoramento-da-qualidade-do-ar-monitorar?orderBy=Data

Stan Development Team. n.d. Stan Reference Manual, Version 2.23. ed.

Teixeira MG, Costa M da CN, Barreto F, Barreto ML. 2009. Dengue: twenty-five years since reemergence in Brazil. *Cadernos de Saúde Pública* **25**:S7–S18. doi:10.1590/S0102-311X2009001300002

medRxiv preprint doi: https://doi.org/10.1101/2020.06.08.20125757; this version posted June 9, 2020. The copyright holder for this preprint (which was not certified by peer review) is the author/funder, who has granted medRxiv a license to display the preprint in perpetuity. It is made available under a CC-BY 4.0 International license .

Teixeira TR de A, Cruz OG. 2011. Spatial modeling of dengue and socio-environmental indicators in the city of Rio de Janeiro, Brazil. *Cadernos de Saúde Pública* **27**:591–602. doi:10.1590/S0102-311X2011000300019

The R Foundation for Statistical Computing. 2020. R. The R Foundation.

Vehtari A, Gelman A, Gabry J. 2017. Practical Bayesian model evaluation using leave-one-out cross-validation and WAIC. *Statistics and Computing* **27**:1413–1432. doi:10.1007/s11222-016-9696-4

Watanabe S. 2010. Asymptotic Equivalence of Bayes Cross Validation and Widely Applicable Information Criterion in Singular Learning Theory 24.

WHO. 2017. Chikungunya. *World Health Organization*. http://www.who.int/news-room/fact-sheets/detail/chikungunya

Wickham H. 2016. ggplot2: Elegant Graphics for Data Analysis. Springer-Verlag.

Wickham H, RStudio. 2017. tidyverse: Easily Install and Load the “Tidyverse.”

World Meteorological Organization, editor. 2007. Guide to the global observing system, 3rd ed. ed, WMO. Geneva: World Meteorological Organization.

Xavier DR, Magalhães M de AFM, Gracie R, Reis IC dos, Matos VP de, Barcellos C. 2017. Difusão espaço-tempo do dengue no Município do Rio de Janeiro, Brasil, no período de 2000-2013. *Cadernos de Saúde Pública* **33**. doi:10.1590/0102-311x00186615

medRxiv preprint doi: https://doi.org/10.1101/2020.06.08.20125757; this version posted June 9, 2020. The copyright holder for this preprint (which was not certified by peer review) is the author/funder, who has granted medRxiv a license to display the preprint in perpetuity. It is made available under a CC-BY 4.0 International license .

Supplementary Material

Figure 1. Meteorological weather stations (red dots) in the 500m X 500m grid and neighbourhoods, Rio de Janeiro city, Brazil.

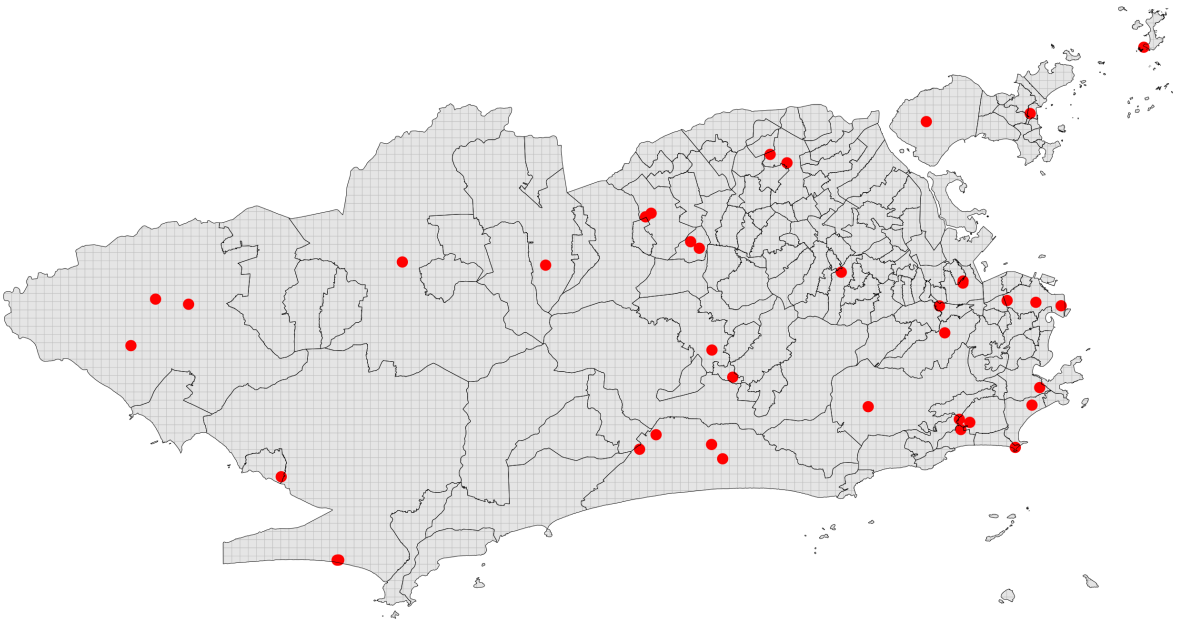

medRxiv preprint doi: https://doi.org/10.1101/2020.06.08.20125757; this version posted June 9, 2020. The copyright holder for this preprint (which was not certified by peer review) is the author/funder, who has granted medRxiv a license to display the preprint in perpetuity. It is made available under a CC-BY 4.0 International license .

Figure 2. Correlation between the spatial effects (in the log scale) of Model 0 versus Model 4, by neighbourhood, weeks 9 to 52 2016, Rio de Janeiro city, Brazil.

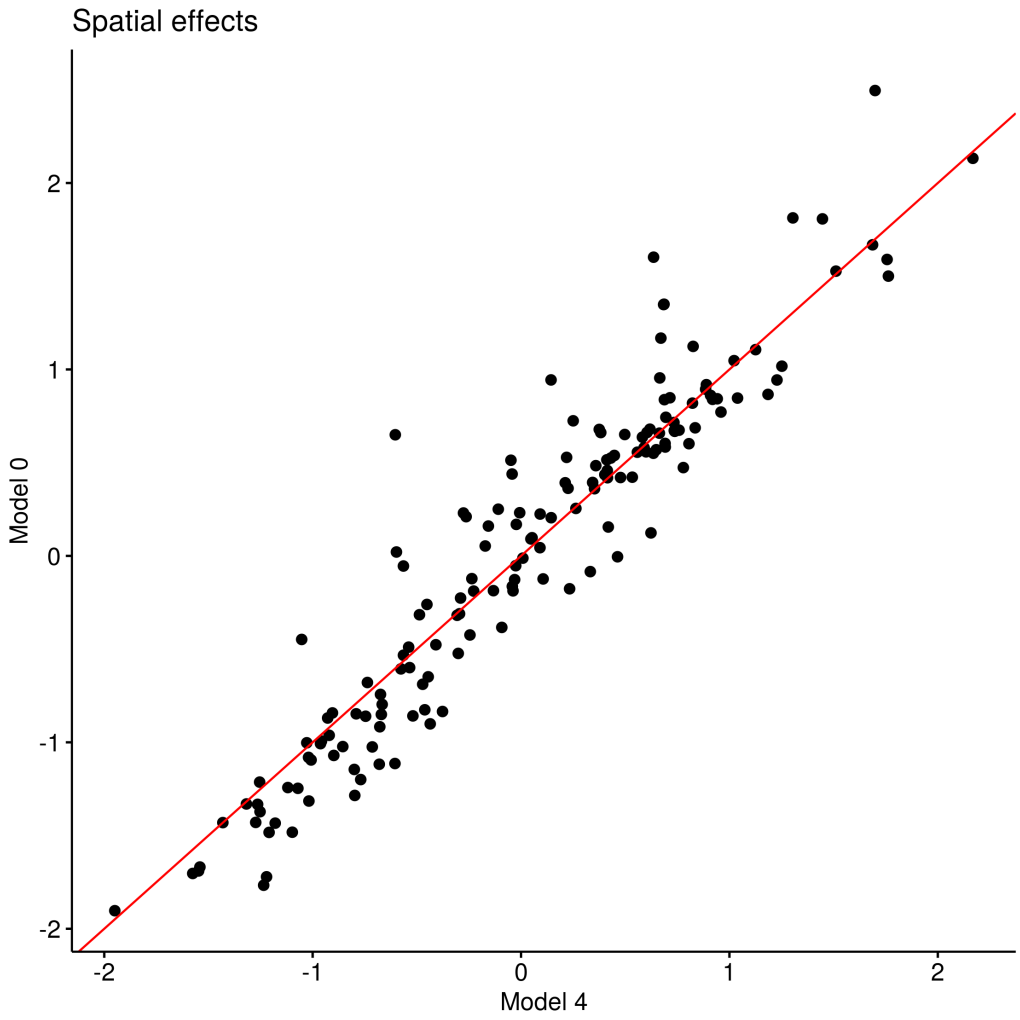

medRxiv preprint doi: https://doi.org/10.1101/2020.06.08.20125757; this version posted June 9, 2020. The copyright holder for this preprint (which was not certified by peer review) is the author/funder, who has granted medRxiv a license to display the preprint in perpetuity. It is made available under a CC-BY 4.0 International license .

Figure 3. Impulse response of the minimum temperature, posterior mean and 90% credible interval, by neighbourhood, Rio de Janeiro city, Brazil.

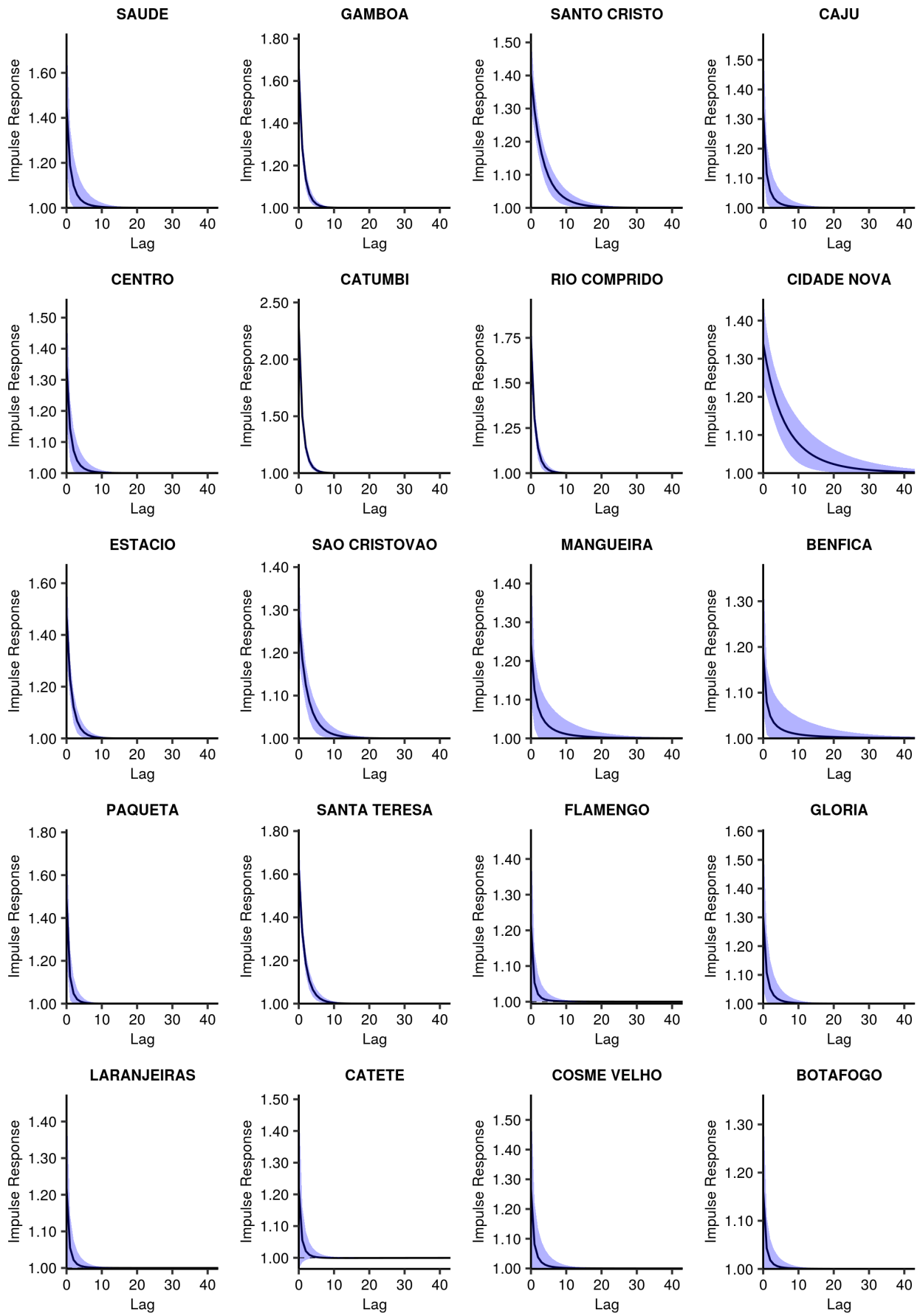

medRxiv preprint doi: https://doi.org/10.1101/2020.06.08.20125757; this version posted June 9, 2020. The copyright holder for this preprint (which was not certified by peer review) is the author/funder, who has granted medRxiv a license to display the preprint in perpetuity. It is made available under a CC-BY 4.0 International license .

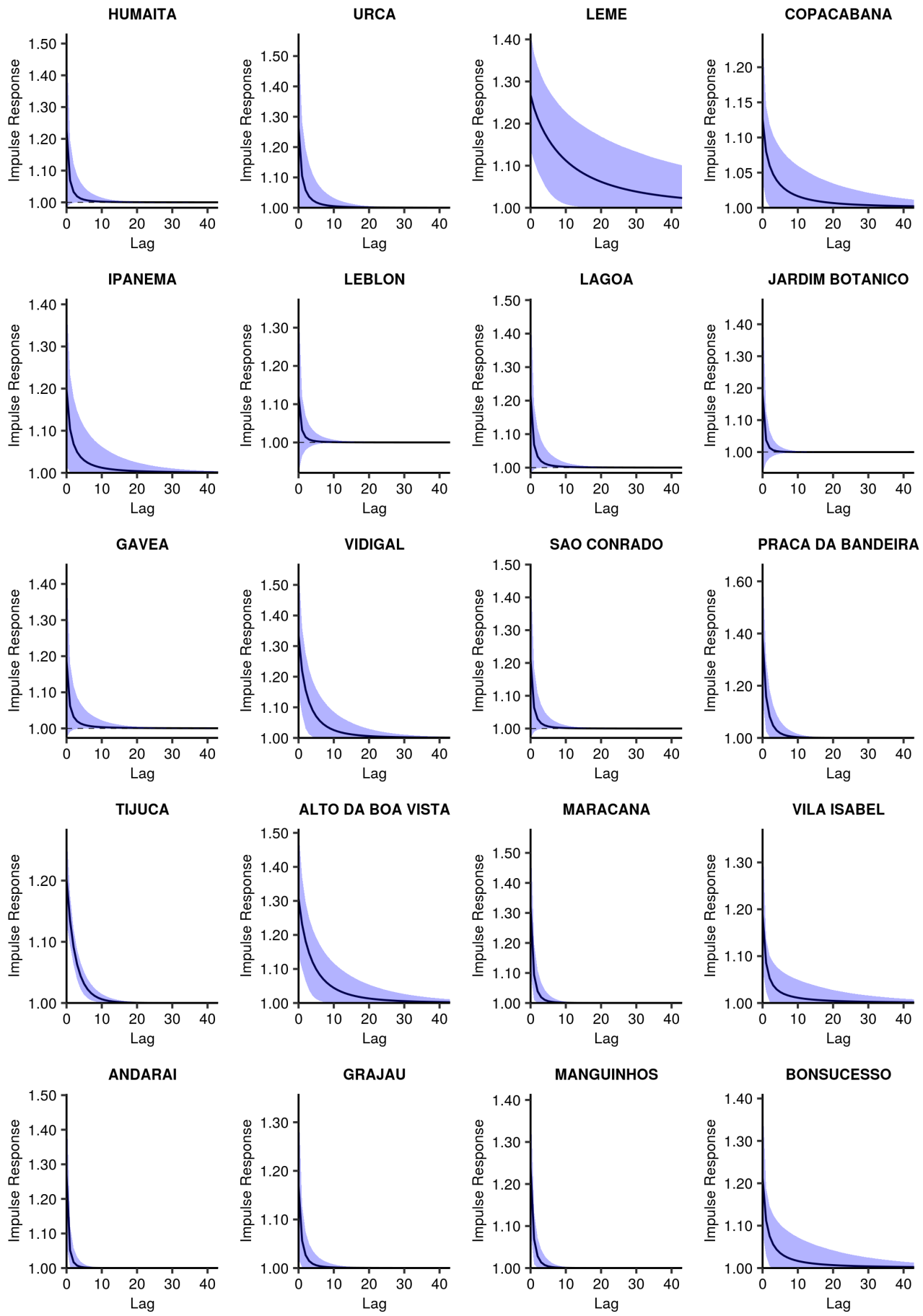

medRxiv preprint doi: https://doi.org/10.1101/2020.06.08.20125757; this version posted June 9, 2020. The copyright holder for this preprint (which was not certified by peer review) is the author/funder, who has granted medRxiv a license to display the preprint in perpetuity. It is made available under a CC-BY 4.0 International license .

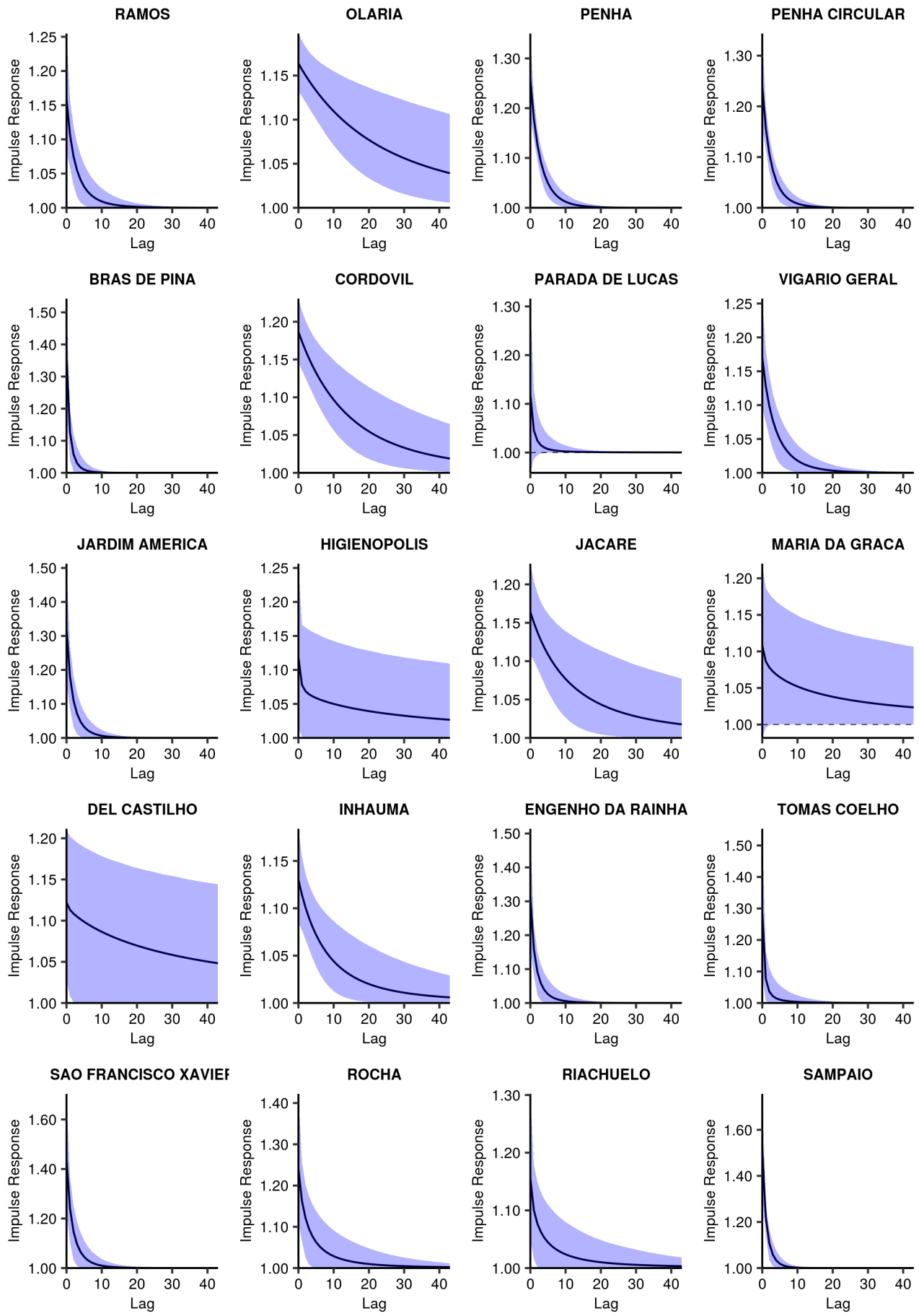

medRxiv preprint doi: https://doi.org/10.1101/2020.06.08.20125757; this version posted June 9, 2020. The copyright holder for this preprint (which was not certified by peer review) is the author/funder, who has granted medRxiv a license to display the preprint in perpetuity. It is made available under a CC-BY 4.0 International license .

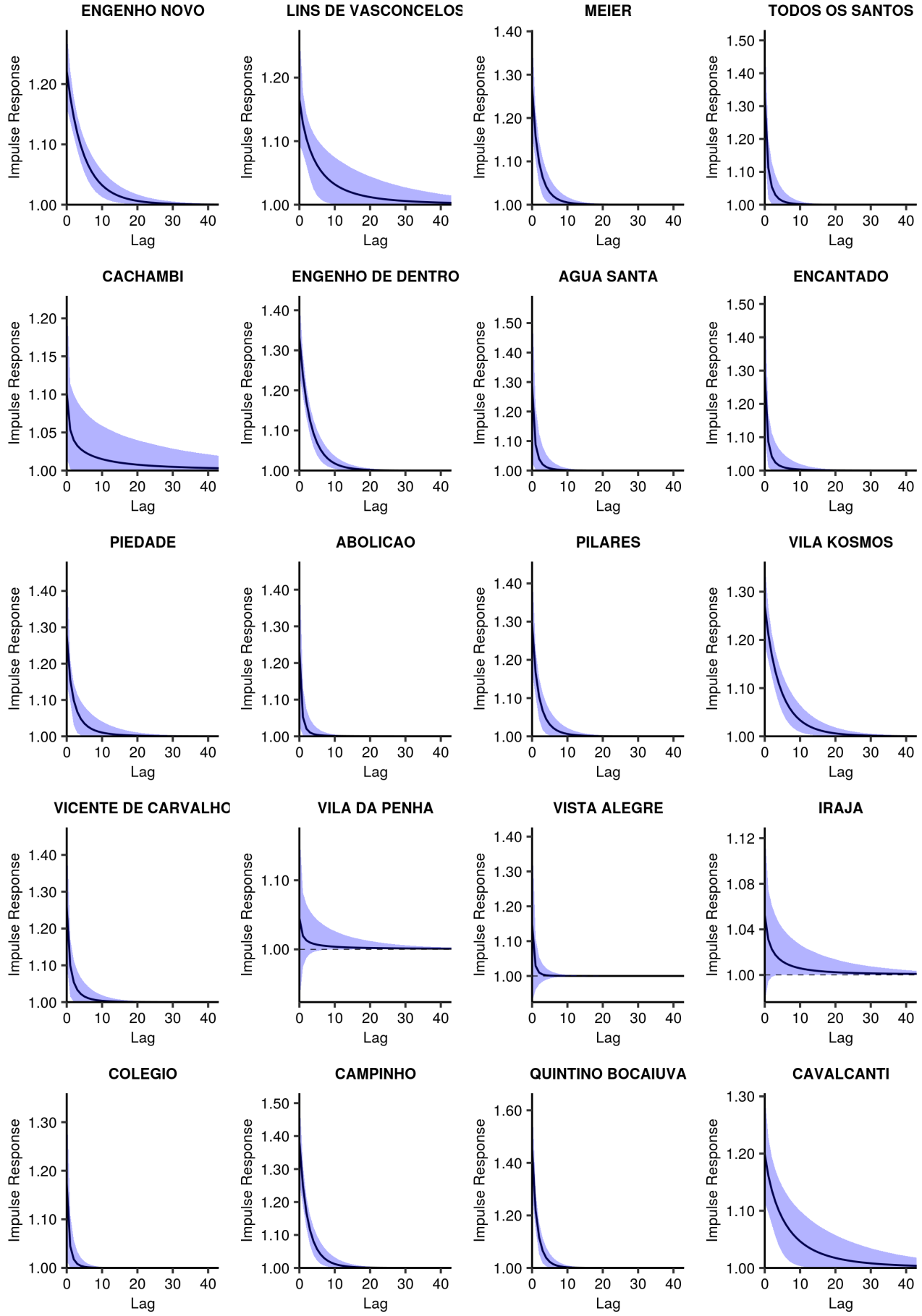

medRxiv preprint doi: https://doi.org/10.1101/2020.06.08.20125757; this version posted June 9, 2020. The copyright holder for this preprint (which was not certified by peer review) is the author/funder, who has granted medRxiv a license to display the preprint in perpetuity. It is made available under a CC-BY 4.0 International license .

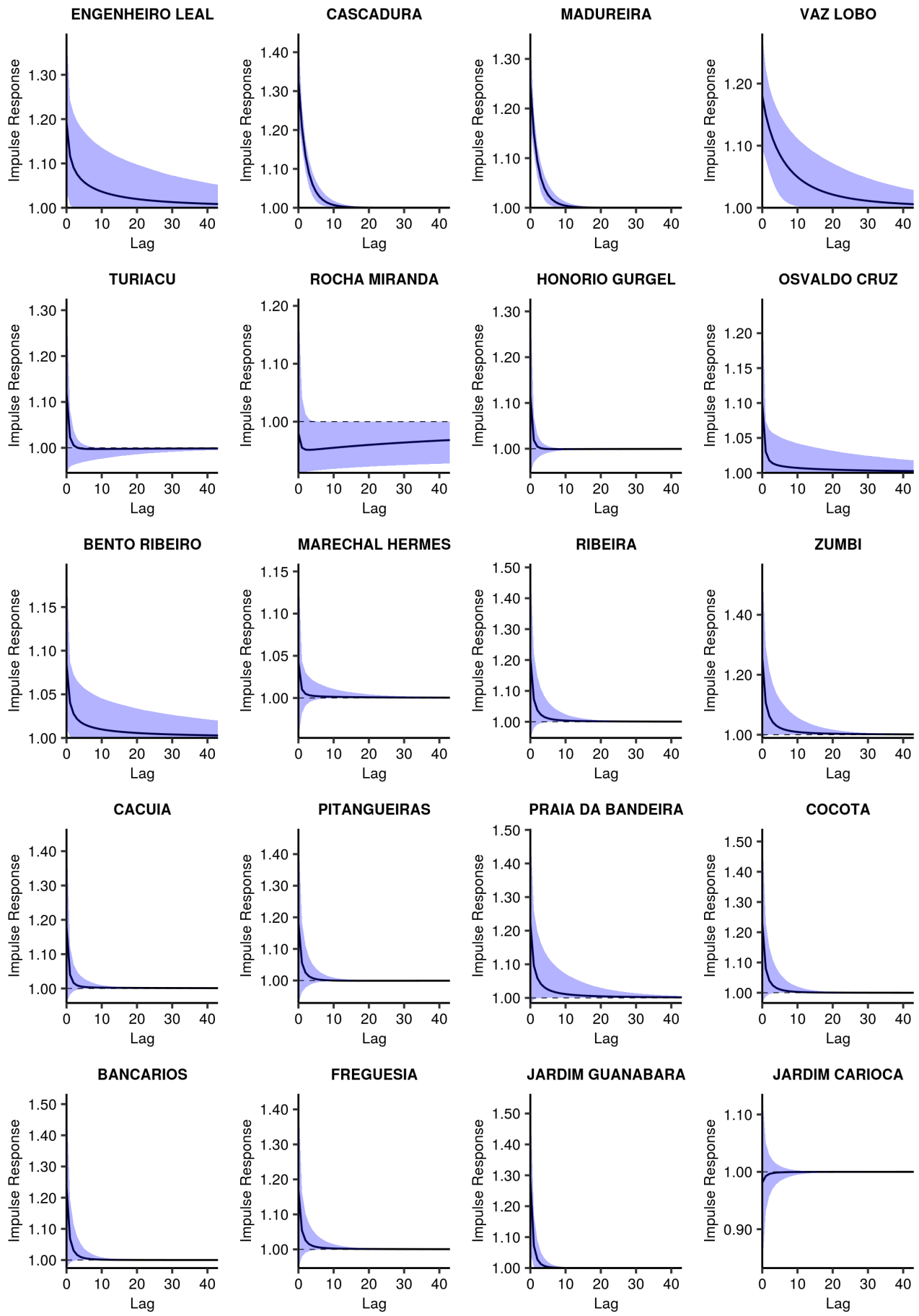

medRxiv preprint doi: https://doi.org/10.1101/2020.06.08.20125757; this version posted June 9, 2020. The copyright holder for this preprint (which was not certified by peer review) is the author/funder, who has granted medRxiv a license to display the preprint in perpetuity. It is made available under a CC-BY 4.0 International license .

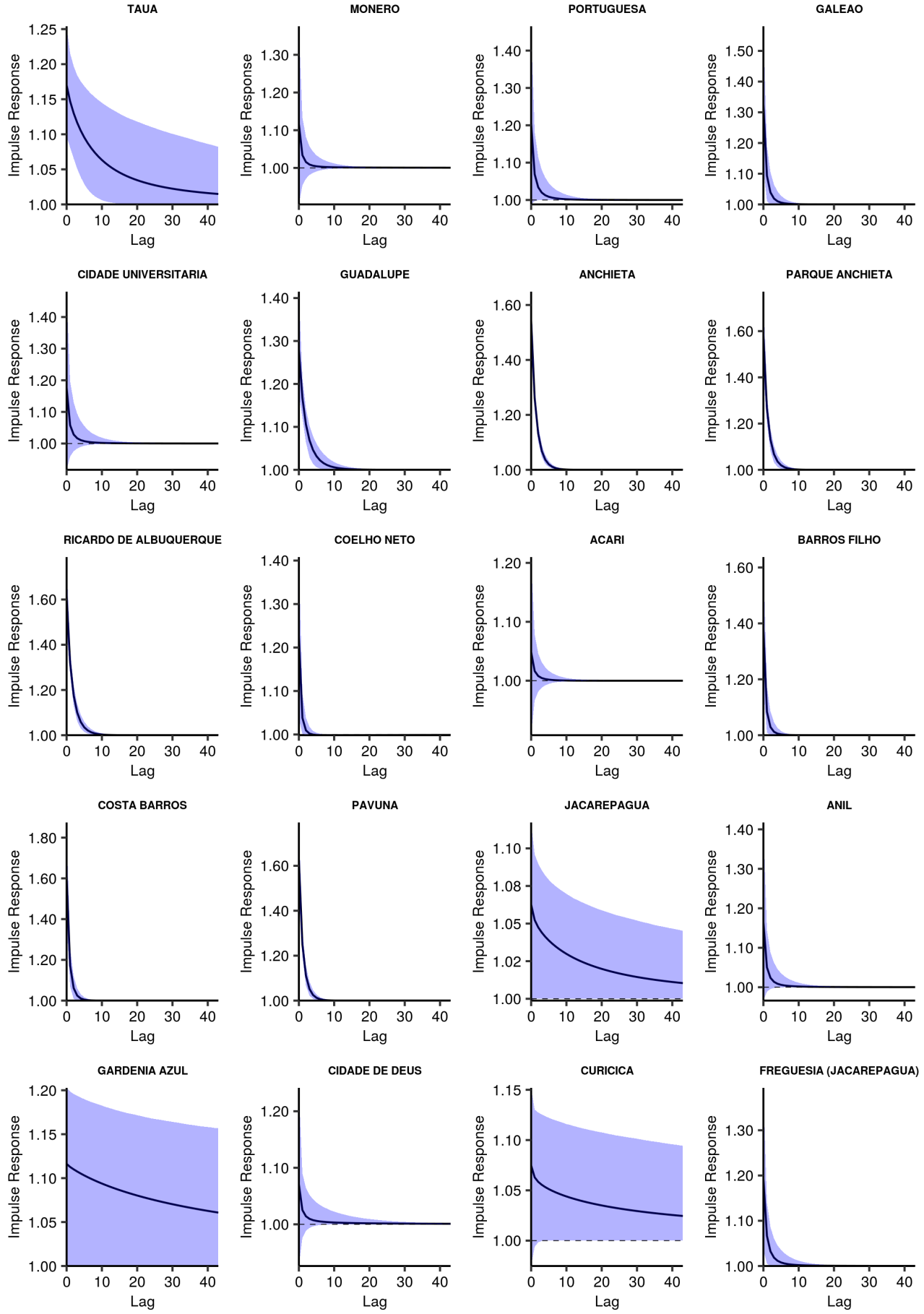

medRxiv preprint doi: https://doi.org/10.1101/2020.06.08.20125757; this version posted June 9, 2020. The copyright holder for this preprint (which was not certified by peer review) is the author/funder, who has granted medRxiv a license to display the preprint in perpetuity. It is made available under a CC-BY 4.0 International license .

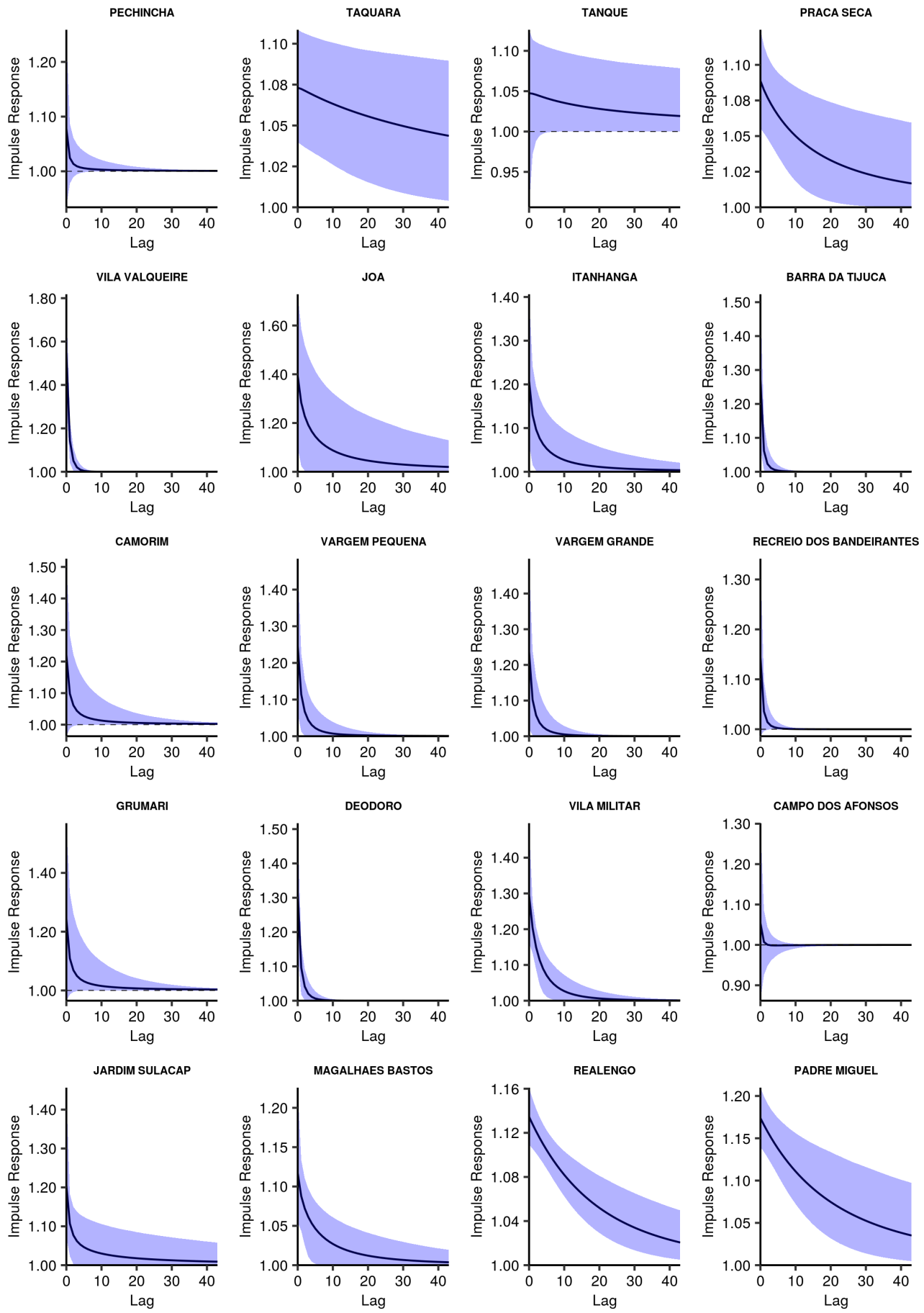

medRxiv preprint doi: https://doi.org/10.1101/2020.06.08.20125757; this version posted June 9, 2020. The copyright holder for this preprint (which was not certified by peer review) is the author/funder, who has granted medRxiv a license to display the preprint in perpetuity. It is made available under a CC-BY 4.0 International license .

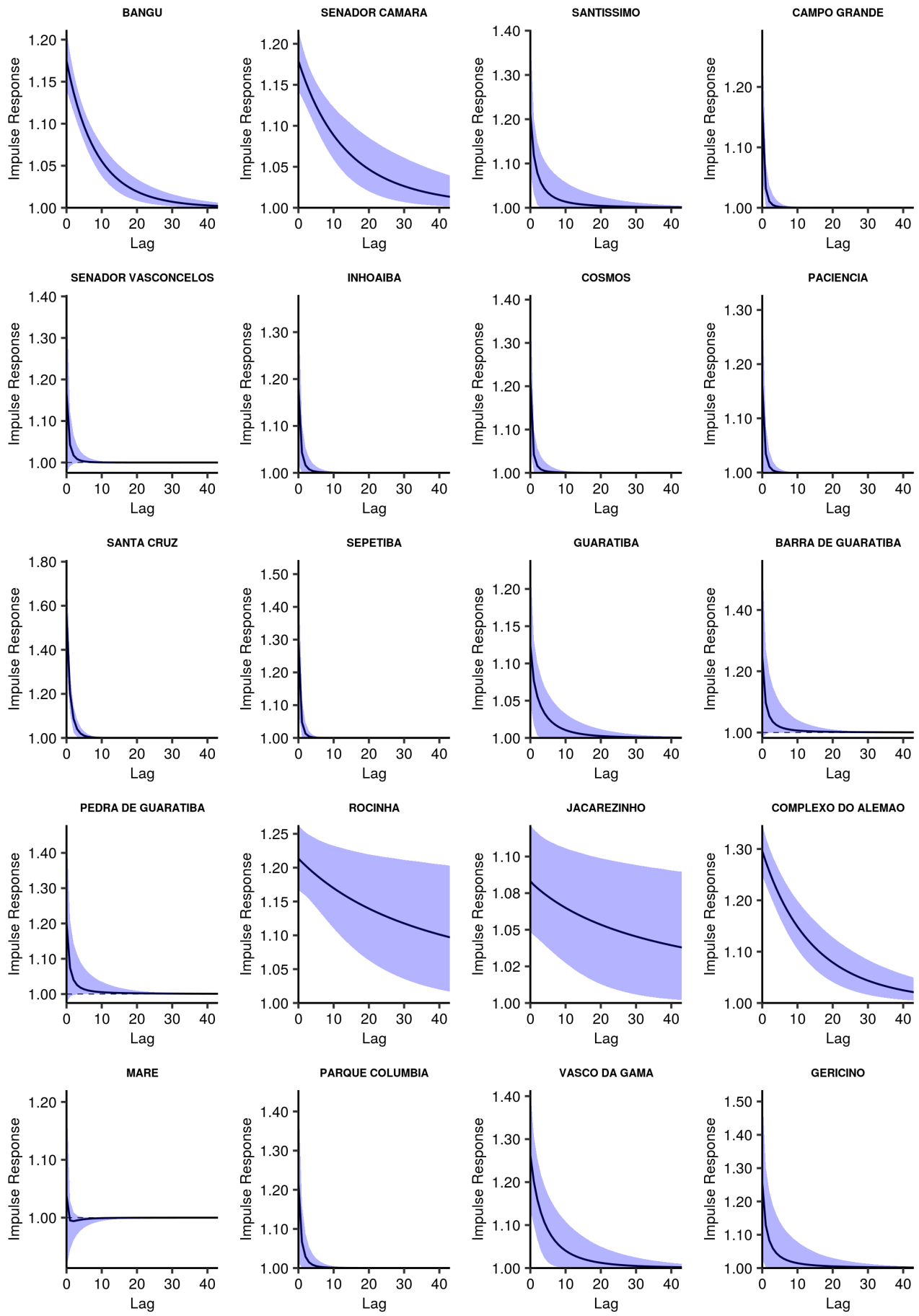
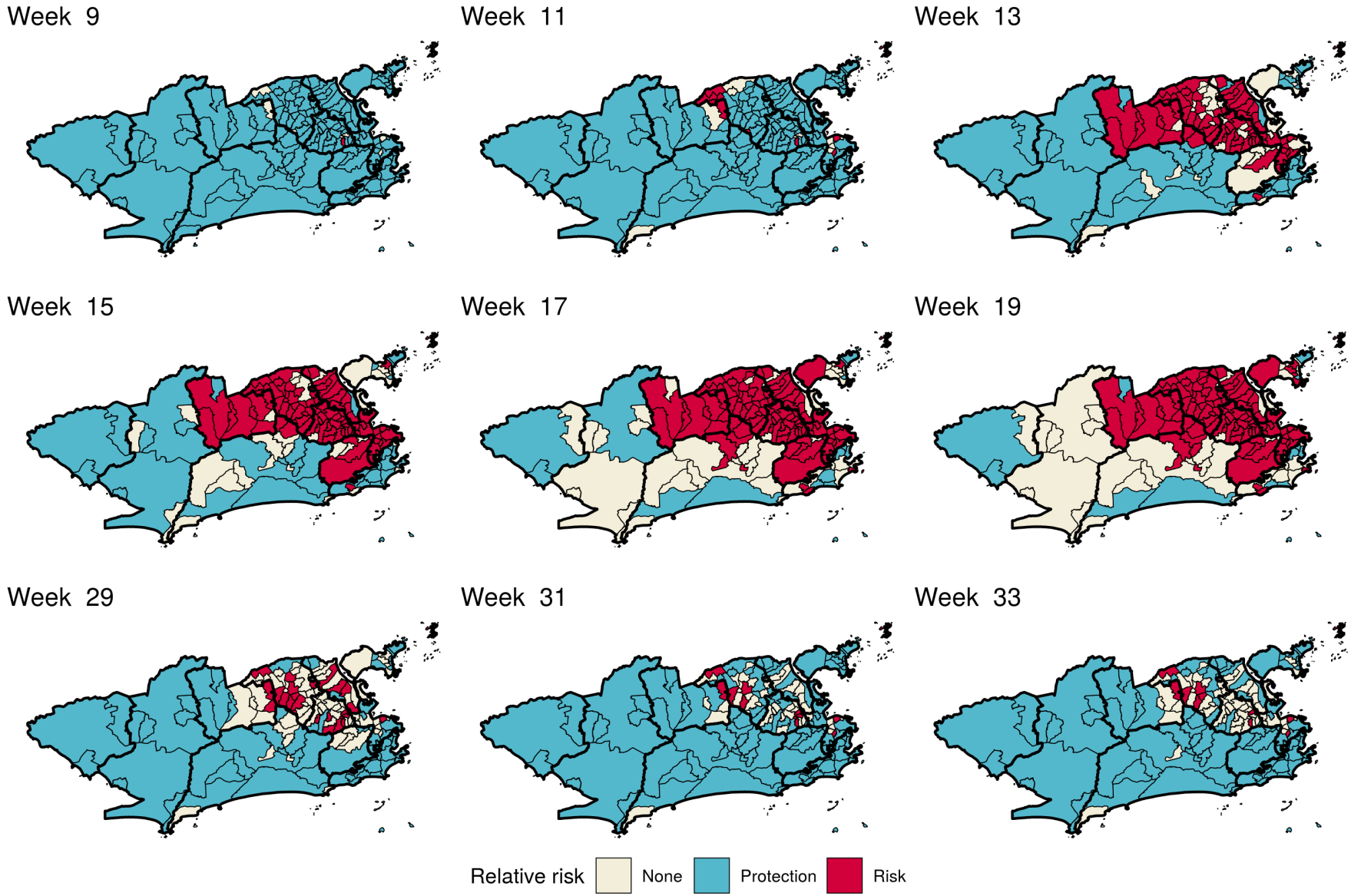
Figure 4. Classification of the chikungunya relative risk by neighbourhood based on the 90% credible interval, selected weeks, Rio de Janeiro city, Brazil.